Journal of Japan Association for Earthquake Engineering, Vol. 23, No. 3, 2023

ANALYSIS OF CORRELATION COEFFICIENTS BETWEEN TWO ORTHOGONAL COMPONENTS OF STRONG-MOTION RECORDS

Makoto TAKAO[1] and Hiroaki SATO[2]

[1] Member, Dr. Eng., General Manager, Atomic Energy Association,
Tokyo, Japan, takaom@atena-j.jp
[2] Dr. Eng., Senior Research Scientist, Central Research Institute of Electric Power Industry,
Chiba, Japan, hiroakis@criepi.denken.or.jp

ABSTRACT: With regard to horizontal components in seismic design of nuclear facilities in Japan when input ground motions are generated based on response spectrum, simulated ground motions composed of two mutually orthogonal components are generated for one target response spectrum. In such a case, the characteristics of the two ground motions are distinguished by the randomness of the phase angle given by the uniformly distributed random numbers and/or the difference in the phase characteristics of the two different components of the observation records. On the other hand, US Nuclear Regulatory Commission standards state that, when performing seismic response analysis for nuclear facilities using the method of simultaneous input of three earthquake ground motion components, the three components should be shown to be statistically independent of each other, and an absolute value for correlation coefficient as proposed by Chen (1975) is introduced as a criterion. In this paper, focusing on the correlation coefficient by Chen (1975), we found the correlation coefficients between two orthogonal components in records of observed strong motions in Japan after 2000, and performed statistical analyses of these correlation coefficients, then analyzed the impact of various earthquake-related parameters upon them. In addition, we actually generated simulated ground motions via a common practice based on the response spectrum and analyzed their correlation coefficients.

Keywords: *Correlation coefficient, Statistical independency, Input ground motion, Statistical analysis, Non-exceedance probability, Elliptical component of polarization*

1. INTRODUCTION

The design basis earthquake ground motions, which are used as input ground motions for nuclear power facilities in Japan, are prepared by either the method based on response spectrum[1), 2)] or the method based on fault models [for example 3)], or both. The response spectrum-based method is based on knowledge obtained from statistical analysis of observation records and is generated by superposition of sinusoidal waves to meet the target response spectrum and other conditions, such as duration, envelope curve, and

phase characteristics[1), 2)]. With this method, for example, two orthogonal horizontal components of ground motions are generated from a single target response spectrum. Therefore, for each ground motion to be generated, phase characteristics from different directional components of the actual ground motion and/or phase characteristics based on uniformly distributed random numbers are applied to generate seismic ground motions with different characteristics.

According to USNRC Regulatory Guide 1.92 (hereinafter referred to as USNRC[4)]), when conducting seismic response analysis of nuclear facilities by simultaneously inputting three components of earthquake motion based on response spectra for seismic design of nuclear facilities, it should be shown that the three components of input ground motions are statistically independent from each other. For example, Chen[5)] refers to the combination method or statistical independence of the input ground motions. In this paper, it is recommended that the absolute value of correlation coefficient (varying from 0 to 1) of input ground motions should be 0.16 or less in the case of simultaneous input of three components. Therefore, the USNRC[4)] cites Chen[5)] and stipulates that the absolute value of the correlation coefficient of input ground motions should not exceed 0.16 in the case of the simultaneous input of three components. Recently, in Japan as well, the correlation coefficient for input ground motions has been introduced in the "ATENA 20-NE01 (Rev. 0) Design Guidelines for Base Isolation Structures, Severe Accident Facilities"[6)] established by the Atomic Energy Association (ATENA), citing USNRC[4)]. The correlation coefficient introduced by Chen[5)] is an indicator that measures the strength of the linear relationship between two components of orthogonal ground motions throughout the time-history waveform, and a large correlation coefficient corresponds to ground motions that move in a certain direction and a small correlation coefficient corresponds to ground motions that vibrate in all directions (see Appendix).

In Japan, there are no examples of analyses related to correlation coefficients using domestic ground motion records, and as far as the authors know, there are no standards that specify correlation coefficients between two orthogonal components of input ground motions except the above-mentioned ATENA guidelines. In recent years, however, there have been reports that, when generating ground motions of two directions based on a single response spectrum, observation records have been evaluated using the elliptical component of polarization (P_E) proposed by Vidale[7)] in order to generate waveforms so that the orbit of the two horizontal components will be on a circle[8), 9)]. In addition, the P_E is qualitatively inversely related to the correlation coefficient, since the P_E becomes 0 when the orbit is on a straight line and becomes 1 when the orbit is on a circle.

In this study, we found the correlation coefficient by Chen[5)] and the absolute values of correlation coefficient used in USNRC[4)] and others for 19 domestic strong-motion records with Japan Meteorological Agency (JMA) seismic intensity of "6 Upper" and "7" from 2000 to 2020 and used statistical analysis to comprehend the basic characteristics of the correlation coefficients between two orthogonal components in domestic strong-motion records. In this study, we also devised a method to use the maximum of the correlation coefficients obtained by rotating the coordinate axes of the two orthogonal components and analyzed the effects of various basic parameters of earthquakes and observation stations, such as magnitude, hypocentral distance and elastic wave velocity of the ground at the observation station, on the correlation coefficient. Furthermore, the correlation coefficients of several combinations of simulated ground motions were analyzed by adopting a method where simulated ground motions are generated based on a generic response spectrum with phase angles determined by uniformly distributed random numbers. Finally, we calculated the above-mentioned elliptical component of polarization P_E of the strong-motion records and the simulated ground motions used in the correlation coefficient study and examined the correspondence with the correlation coefficient devised in this study. To the best of the authors' knowledge, there has been no study focusing on the relationship between the correlation coefficient and P_E. In addition, our analyses were conducted using the Cartesian components, keeping in mind that the correlation coefficients are used as a reference in the development of design basis earthquake ground motions in seismic design, since the Cartesian coordinate system (x, y, z) has two or three components in general seismic design, not limited to that of nuclear facilities.

2. STRONG-MOTION RECORDS AND SIMULATED GROUND MOTION UNDER CONSIDERATION

2.1 Underground strong-motion records by NIED (KiK-net)

The JMA Seismic Intensity Database Search was used to search for earthquakes that recorded an intensity of "6 Upper" and "7" on the JMA seismic intensity scale from 2000 to 2020. The reason for selecting "6 Upper" and "7" is that the design basis earthquake ground motions used in seismic design for nuclear facilities are strong motions defined as those occurring on solid ground with a shear wave velocity (Vs) of 700 m/s or more (hereinafter referred to as "free rock surface").

As a result of the search, 19 earthquakes were selected as shown in Table 1. The correlation coefficients for the 19 selected earthquakes were analyzed using the acceleration records at the bottom of the boreholes (hereinafter referred to as "underground") of KiK-net[10], which is a strong-motion seismograph network of the National Research Institute for Earth Science and Disaster Resilience (NIED). The reason for using the underground acceleration records is to clarify the comparison and investigation based on the fact that the design basis earthquake ground motions for nuclear facilities are defined as occurring on solid ground with Vs of 700 m/s or more, as mentioned above.

For the 19 earthquakes, we selected observation stations within a radius of 50 km from the epicenter to ensure sufficient statistical data and to prevent the seismic records from becoming too small due to distance attenuation characteristics. As for the three subduction-zone earthquakes No.9, No.10 and No.13 in Table 1, however, there were no stations within 50 km of the epicenter. Therefore, we decided to use records from the top 10 stations in ascending order from the epicenter distance. As a result, a total of 166 (accumulated number) three-component records were used. Table 1 shows the breakdown of the number of observations for each earthquake analyzed. As described in Section 3.1, Chen[5] analyzed acceleration records of 129 stations, and the total number of 166 stations treated in this paper is equivalent to or greater than that of the previous study.

Table 1 Earthquakes analyzed for correlation coefficient (KiK-net)

No.	Date	Time	Epicentral area	Mj	Maximum JMA seismic intensity	Maximum acceleration (Gal)*	Number of stations for analysis
1	2000/10/06	13:30:18	Western Tottori Pref.	7.3	6 Upper	654	10
2	2003/07/26	07:13:31	Central Miyagi Pref.	6.4	6 Upper	101	5
3	2004/10/23	17:56:00	Chuetsu, Niigata Pref.	6.8	7	497	8
4	2004/10/23	18:11:57	Chuetsu, Niigata Pref.	6.0	6 Upper	210	9
5	2004/10/23	18:34:06	Chuetsu, Niigata Pref.	6.5	6 Upper	354	9
6	2007/03/25	09:41:58	Offshore Noto Peninsula	6.9	6 Upper	257	1
7	2007/07/16	10:13:22	Offshore Jo-Chuetsu, Niigata Pref.	6.8	6 Upper	88	5
8	2008/06/14	08:43:45	Southern inland, Iwate Pref.	7.2	6 Upper	1078	14
9	2011/03/11	14:46:18	Offshore Sanriku	9.0	7	221	10
10	2011/03/11	15:15:34	Offshore Ibaraki Pref.	7.6	6 Upper	98	10
11	2011/03/12	03:59:16	Northern Nagano Pref.	6.7	6 Upper	125	12
12	2011/03/15	22:31:46	Eastern Shizuoka Pref.	6.4	6 Upper	49	17
13	2011/04/07	23:32:43	Offshore Miyagi Pref.	7.2	6 Upper	208	10
14	2016/04/14	21:26:34	Kumamoto, Kumamoto Pref.	6.5	7	288	8
15	2016/04/15	00:03:46	Kumamoto, Kumamoto Pref.	6.4	6 Upper	150	8
16	2016/04/16	01:25:05	Kumamoto, Kumamoto Pref.	7.3	7	287	7
17	20160/4/16	03:55:53	Aso, Kumamoto Pref.	5.8	6 Upper	86	10
18	2018/09/06	03:07:59	Middle East Iburi, Hokkaido	6.7	7	261	10
19	2019/06/18	22:22:20	Offshore Yamagata Pref.	6.7	6 Upper	107	3
Total (accumulated number)							166

* Square root of the sum of the squares of the three components, where Gal is cm/s^2.

2.2 Strong-motion records on outcropped bedrock by CRIEPI

It has already been mentioned that this paper is based on the KiK-net underground records, since the design basis earthquake ground motions for nuclear facilities are defined at free rock surface. However, although the KiK-net underground records are equivalent or better than the free rock surface in terms of shear wave velocity, they are seismic motions that may include reflected waves (so-called E + F waves), not waves on outcropped bedrock (so-called 2E waves), which are defined as an input ground motion. Therefore, in order to confirm whether or not there is a difference in the characteristics of the correlation coefficients between E + F waves and 2E waves, we also examined the observation records of the strong-motion observation network on outcropped bedrock (RK-net)[11] of the Central Research Institute of Electric Power Industry (CRIEPI).

The earthquakes in Table 1 for which there are observation records by RK-net were considered. The radius from the epicenter was expanded to 100 km, compared to general rule of 50 km for KiK-net, in order to increase the data as much as possible. As a result, 19 records of the 5 earthquakes shown in Table 2 were selected to be analyzed. In addition, P-wave velocities (Vp) at the 19 stations ranged from 1.81 to 5.87 km/s, and S-wave velocities (Vs) ranged from 0.86 to 3.36 km/s (shown as minimum to maximum).

Table 2 Earthquakes analyzed for correlation coefficient (RK-net)

No.	Date	Time	Epicentral area	Mj	Maximum JMA seismic intensity	Maximum acceleration (Gal)*	Number of stations for analysis
8	2008/06/14	08:43:45	Southern inland, Iwate Pref.	7.2	6 Upper	94	1
11	2011/03/12	03:59:16	Northern Nagano Pref.	6.7	6 Upper	8	1
12	2011/03/15	22:31:46	Eastern Shizuoka Pref.	6.4	6 Upper	168	15
18	2018/09/06	03:07:59	Middle East Iburi, Hokkaido	6.7	7	21	1
19	2019/06/18	22:22:20	Offshore Yamagata Pref.	6.7	6 Upper	129	1
Total							19

* Square root of the sum of the squares of the three components

2.3 Generation of simulated ground motions

Simulated ground motions were generated using the method applied to design of nuclear facilities. The response spectrum of ground motion due to an earthquake whose source cannot be identified in advance as proposed by Kato et al.[12] was applied and the duration and envelope curve were set assuming M7.3 with reference to the Hyogo-ken Nanbu earthquake, and the equivalent hypocentral distance was set to 20 km. Then simulated ground motions were prepared based on JEAG4601-2015[2]. In addition, the phase characteristics were determined using uniformly distributed random numbers, and the time-history waveforms were set at 0.01 second increments. Following these methods, simulated ground motions with duration of about 43 seconds are to be generated, targeting maximum accelerations of 450 Gal and 300 Gal for the horizontal and vertical motions, respectively.

The above method was used to generate 200 horizontal ground motions and 100 vertical ground motions, from which two horizontal motions and one vertical motion were arbitrarily combined to generate 100 different ground motions (100 × 3 components), which were used for the analysis of correlation coefficients.

3. CORRELATION COEFFICIENT ANALYSIS METHOD

3.1 Definition of correlation coefficient

According to the method proposed by Chen[5], the correlation coefficient between two variables (two components of ground motion) is defined by Eq. (1).

$$\rho_{XY} = \frac{\mathrm{cov}(X,Y)}{\sigma_X \sigma_Y} \tag{1}$$

in which ρ_{XY} : correlation coefficient between variables X and Y, $\mathrm{cov}(X,Y)$: covariance of variables X and Y, and σ_X : standard deviation of variable X, σ_Y : standard deviation of variable Y

$$\rho_{XY} = \frac{\sum_{i=1}^{n}(x_i - \bar{x})(y_i - \bar{y})}{\sqrt{\sum_{j=1}^{n}(x_j - \bar{x})^2}\sqrt{\sum_{k=1}^{n}(y_k - \bar{y})^2}} \tag{2}$$

in which x_i : the i-th component of variable X, y_i : the i-th component of variable Y, n : the number of data in variables X and Y, $\bar{x}$: the mean (arithmetic mean) of variable X, and $\bar{y}$: the mean (arithmetic mean) of variable Y.

Chen[5] used three different data sets (104, 12, and 13 points for the first, second, and third sets, respectively) and analyzed correlation coefficients in three different combinations (H1 and H2, H1 and V, and H2 and V) by selecting two components from each set of three-component records for each observation station. Here, H1 and H2 represent the orthogonal axial vibratory components in the horizontal plane, and V represents the vertical component. The mean of the absolute values of the correlation coefficients was calculated for each of the three data sets, and the maximum of the mean of the total of nine data sets (three sets x three combinations) was about 0.16. Therefore, Chen[5] recommended that an absolute value of the correlation coefficient should be 0.16 or less.

In this paper, the x-, y-, and z-axes correspond to the EW, NS, and UD components of the ground motion records, respectively, and three correlation coefficients were calculated from the three components of ground motions at each station: the correlation coefficient between the EW and NS components, the correlation coefficient between the NS and UD components, and the correlation coefficient between the UD and EW components. For the analysis of the correlation coefficients using the KiK-net underground acceleration records, the orientation was corrected according to the explanation of "Installation orientation of KiK-net strong-motion seismograph" available on the website of the NIED[13].

3.2 Points to be considered in calculation of correlation coefficients

The definition of the correlation coefficient is given in Section 3.1. In this paper, however, two criteria are set for the handling of data for analysis of the correlation coefficient. One is a criterion to determine the range of data to be analyzed (acceleration threshold), and the other is a criterion to select wave groups (handling of wave groups) in the case where the wave is composed of multiple wave groups. These are described in detail below.

3.2.1 Acceleration threshold

As can be seen from Eq. (2), the correlation coefficient is calculated using the deviation from the mean

of each component in both the denominator and the numerator, and thus is hardly affected by the near-zero values recorded before and after the seismic waveform (in this paper, the acceleration waveform). Therefore, it can be easily expected that there is no significant difference between calculating the correlation coefficient using all the published time-history waveform or only the main portion of the waveform, excluding the near-zero values. However, from the viewpoint of ensuring objectivity and reproducibility in the analysis of correlation coefficients, it is desirable to establish some criteria for setting the range of data to be analyzed. This is also related to the definition of seismic motion duration, which is generally defined as the time from the first to the last exceedance of a certain threshold[14), 15)] or defined based on the cumulative value of the square (power) of the observation records in time-history[16)]. In this study, the former method was referred to and the following procedure was applied for the analysis.

Step 1: Confirm the mainshock (or main portion) of the time-history waveform of the KiK-net underground record, and visually read the start and end points of the analysis section in units of 10 seconds (setting of the search section).

Step 2: Adopt 1% of the maximum of the root-mean-square of the three acceleration components in the search section tentatively set in Step 1 as a threshold value.

Step 3: In the search section set in Step 1, extract the section where the time-history of the root-mean-square of the three acceleration components exceeds the threshold value set in Step 2 (setting of the adopted section).

Step 4: Calculate the correlation coefficient using the record of the adopted section set in Step 3.

As a specific example of analysis using the above procedure, an explanation is given of TTRH02 (Hino), the observation station with the shortest epicenter distance for earthquake No. 1 in Table 1. Figure 1 shows the acceleration time-history waveform at TTRH02. In Step 1, the search section was set from 10 to 100 seconds. In Step 2, the threshold value was set at 6.536 Gal, which is 1% of the maximum of the root-mean-square of the three acceleration components. In Step 3, the time between 14.445 seconds and 93.895 seconds, which exceeded 6.536 Gal in the search section of 10 seconds to 100 seconds, was set as the adopted section. In Step 4, the correlation coefficients for the adopted section set in Step 3 were analyzed.

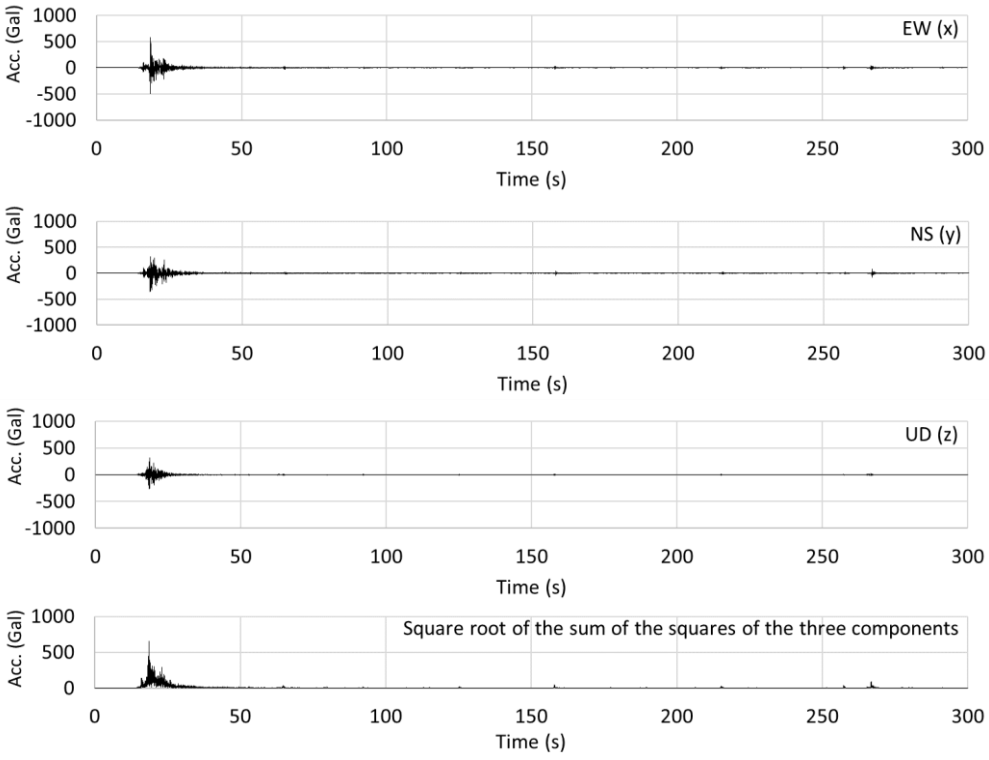

Fig. 1 Acceleration time-history waveforms of TTRH020010061330

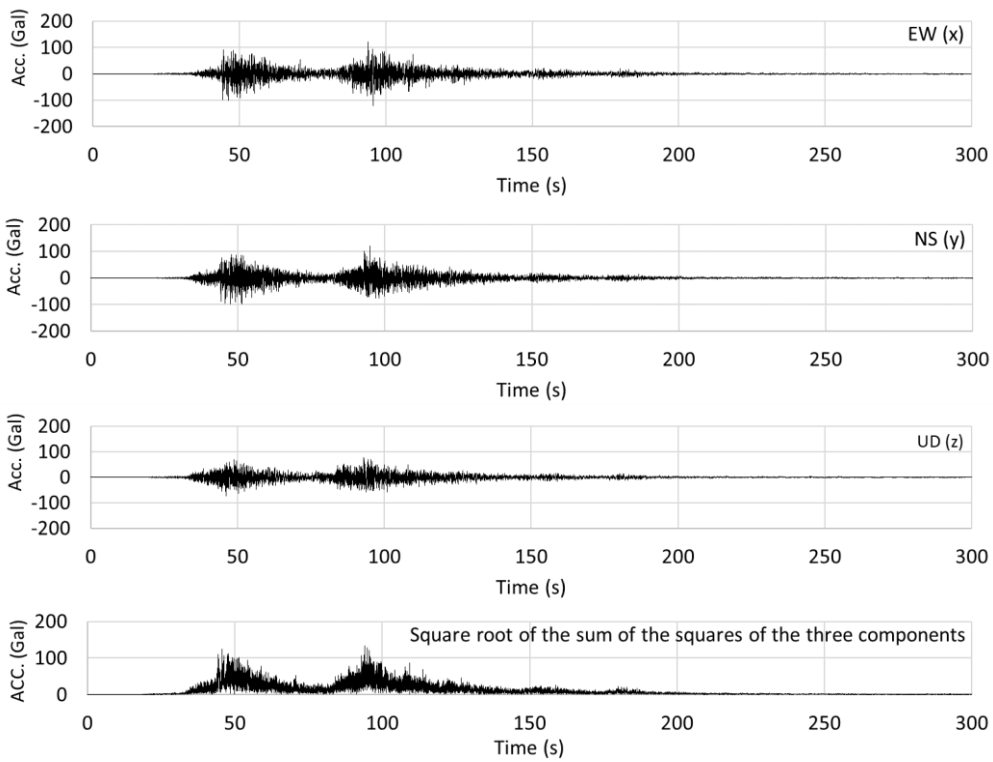

Fig. 2 Acceleration time-history waveforms of MYGH041103111446

Table 3 shows the effect of the analysis section on the correlation coefficient, using TTRH02 as an example. Case (1) is the correlation coefficient when all data are used, case (2) is the correlation coefficient when data set as the search section are used, and case (3) is the correlation coefficient when data from the section that satisfies the threshold value obtained as a result of the search (adopted section) are used. In Table 3 and similar comparison tables (Table 4 and Table 12), the data are shown to the fifth decimal place for the sake of comparison, while in the other tables, the data are shown to the third decimal place.

As Table 3 shows, the effect of the analysis section on the correlation coefficient is extremely small in terms of whether it contains zero or near-zero data. However, as mentioned above, from the viewpoint of objectivity and reproducibility of the analysis results, it is desirable to conduct the analysis with criteria such as those in steps 1 through 4, so the above procedures were adopted.

Table 3 Effect of analysis section

Analysis section	EW-NS (x-y)	NS-UD (y-z)	UD-EW (z-x)
case (1) 0–299.995 s (all data)	−0.05422	0.18734	−0.14787
case (2) 10–100 s (search section)	−0.05506	0.18589	−0.14676
case (3) 14.445–93.895 s (adopted section)	−0.05504	0.18591	−0.14680

3.2.2 Handling of wave groups

Since the source process of the 2011 off the Pacific coast of Tohoku Earthquake, No. 9 in Table 1, is complicated [for example 17)], most of its observation records consist of two major wave groups. As an example, Fig. 2 shows the acceleration records of MYGH04 (Towa). In Section 4.2, the relationship between the correlation coefficient and the difference in occurrence time of the maximum acceleration of each component are analyzed and discussed. In this case, if both two wave groups are employed in Analysis B, which is detailed in Section 4.3, there is a case that the difference in occurrence time of the maximum acceleration (absolute value in this case) of each component will be obtained across two wave groups. For example, it would be the case that the maximum of the EW component is given by the first wave

group and the maximum of the NS component is given by the second wave group. Nevertheless, the purpose of this paper is to understand the characteristics of correlation coefficients that should be taken into account when generating simulated ground motions that are to be generated by applying design response spectrum, which are widely employed in practice, and considering time-history characteristics of the waveform consisting of one wave group, but not targeting complex waveforms that consist of two wave groups. When considering earthquake ground motions with a complex source process and multiple wave groups in seismic design, it is desirable to generate simulated ground motions using the method based on the fault model described above.

In light of the above, based on the purpose of the study and from the viewpoint of further clarifying consideration of the relationship between the correlation coefficient and the difference in occurrence time of the maximum acceleration of each component, we decided to analyze the correlation coefficient by applying the first wave group for waveforms that consist of two major wave groups. The analysis procedure is basically as described in Section 3.2.1, but for records for which it is difficult to set the end point of step 1 in units of 10 seconds, it was set in units of 5 seconds or 1 second.

Table 4 shows the effect of the analysis section on the correlation coefficients, and it can be seen that there is a clear difference between case (1) and case (3). The correlation coefficient when the second wave group is applied is also shown for reference.

Table 4 Effect of analysis section (effect of wave groups)

Analysis section	EW-NS (x-y)	NS-UD (y-z)	UD-EW (z-x)
case (1) 0–299.99 s (all data)	−0.04065	−0.09330	0.08667
case (2) 20–75 s (search section)	0.02053	−0.11705	0.08972
case (3) 20.76–74.99 s (adopted section)	0.02053	−0.11705	0.08972
Reference: 75.00–259.89 s (second wave group)	−0.08857	−0.07606	0.08470

4. ANALYSIS RESULTS OF ACTUAL GROUND MOTION (STRONG-MOTION RECORDS)

4.1 Analysis results of correlation coefficients and absolute values of correlation coefficients

For each three-component record of a total of 166 observation stations (accumulated number), the correlation coefficients were calculated for the three combinations (EW-NS, NS-UD, and UD-EW) described in Section 3.1, and a total of 498 statistical data were obtained. The absolute values of the correlation coefficients were also calculated following Chen[5] and USNRC[4]. The statistical results of the correlation coefficients and absolute values of the correlation coefficients are shown in Table 5. The histograms of the correlation coefficients and the absolute values of the correlation coefficients are shown in Fig. 3 and Fig. 4, respectively.

As shown in Table 5, the mean of the correlation coefficients is almost zero at −0.004, and Fig. 3 shows that the distribution is approximately normal. Table 6 shows (1) the test of the original data of (i) and the original data of (ii), (2) the test of the original data of (ii) and the original data of (iii) and (3) the test of the original data of (iii) and the original data of (i) in Table 5. The results of the F-test at the 5% significance level (two-tailed) showed that the null hypothesis “population variances are equal” was not rejected for (1) and (2) and was rejected for (3). For this reason, for the t-tests at the 5% significance level (two-tailed), the “t-test on two samples with equal variances” was conducted for (1) and (2), and the “t-test on two samples with unequal variances” was conducted for (3). As a result, the null hypothesis “population means are equal” was not rejected among (i), (ii) or (iii) either, leading to the conclusion that it cannot be said that there are differences among the population means of the data (i), (ii) and (iii). Based on the above, it was decided to judge the results of the F-tests and the t-tests comprehensively, and to integrate (i) through (iii) for discussion. Although omitted for reasons of space, a probability paper check (so-called Q-Q plot) was also performed on the 498 integrated data, and it was confirmed that the correlation coefficients generally follow a normal distribution in the range of −0.3 to 0.3. These results suggest that 498 data for a total of 166 stations are sufficient for statistical processing. It should

be noted that the above are statistical treatments for the case of integrating inland crustal earthquakes and subduction-zone earthquakes, whereas it has been confirmed that there is no significant difference between the results obtained by applying only inland crustal earthquakes and those obtained by integrating the two types of earthquakes.

Figure 4 shows a histogram of the absolute values of the correlation coefficients. Since the correlation coefficients follow a normal distribution with almost zero as the mean, the distribution of absolute values of correlation coefficients is in a form of which the original distribution is folded at zero as a center. Therefore, the standard deviation of the absolute values of the correlation coefficients is not shown in Table 5.

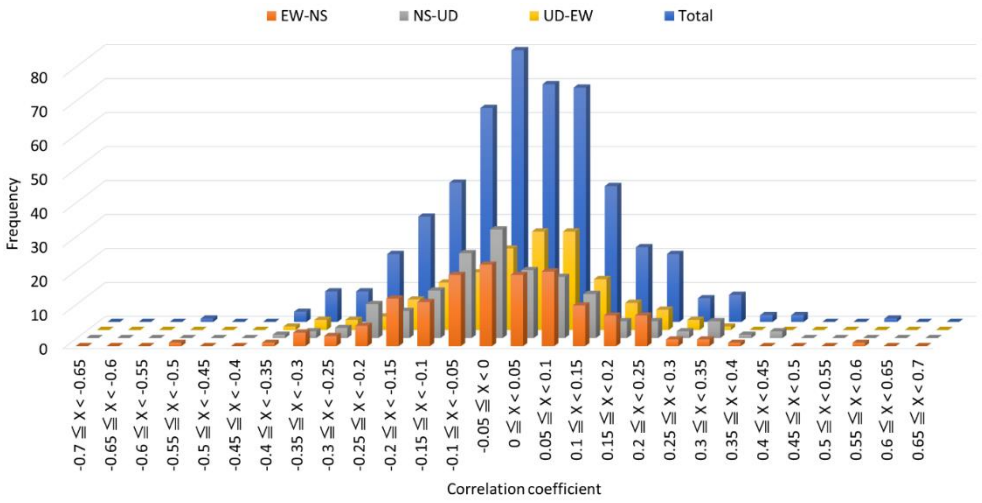

Fig. 3 Histogram of correlation coefficients

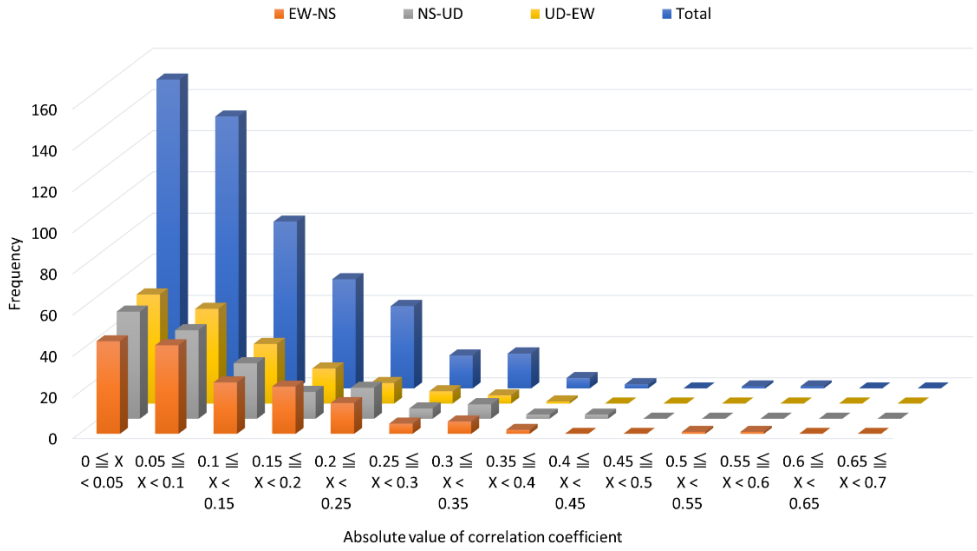

Fig. 4 Histogram of absolute values of correlation coefficients

Next, we discuss the records with the largest and smallest absolute values of the correlation coefficients in Table 5. Information on the records that resulted in the maximum and minimum shown in Table 5 is presented in Table 7, and the relationship diagram of the two components analyzed for correlation coefficients (which, if connected by lines, corresponds to an acceleration orbit) is shown in Figs. 5 and 6. Figures 5(a), 5(b) and 5(c) are records showing the maximums, all of which are characterized by distribution with a major axis in one direction. On the other hand, Figs. 6(a), 6(b) and

6(c), which are the records showing the minimums, show the distribution with no major axis direction as observed in Fig. 5 and it may be seen that two acceleration components of time-history have almost no or low correlation with each other. Note that the adopted sections set in Step 3 of Section 3.2.1 are displayed in Figs. 5 and 6.

For reference, when considering from the viewpoint of comparison with Chen[5)], the mean of the correlation coefficients is –0.004, while Chen[5)] ranges from 0.0029 to 0.0187, and the standard deviation of the correlation coefficient is 0.143, while Chen[5)] ranges from 0.1774 to 0.2116. On the other hand, the mean of the absolute values of correlation coefficients is 0.111, while that of Chen[5)] ranges from 0.1241 to 0.1632, showing no remarkable difference between the two. Here, the values of Chen[5)] are presented as a range from the plural values presented in the paper.

Table 5 Results of statistical analysis of correlation coefficients and absolute values of correlation coefficients (KiK-net, underground)

	Correlation coefficient				Absolute value of correlation coefficient			
	EW-NS (i)	NS-UD (ii)	UD-EW (iii)	Total	EW-NS	NS-UD	UD-EW	Total
Number of data	166	166	166	166 × 3	166	166	166	166 × 3
Mean	−0.005	−0.008	0.001	−0.004	0.120	0.111	0.101	0.111
Standard deviation	0.155	0.145	0.129	0.143	–	–	–	–
Maximum	0.587	0.413	0.313	0.587	0.587	0.413	0.368	0.587
Minimum	−0.546	−0.359	−0.368	−0.546	0.001	0.001	0.004	0.001

Table 6 Results of F-test and t-test

Type of test	Item	(1) test of the original data of (i) and the original data of (ii) in Table 5	(2) test of the original data of (ii) and the original data of (iii) in Table 5	(3) test of the original data of (iii) and the original data of (i) in Table 5
F-test (Two-tailed)	p-value	0.392	0.119	0.016
	Null hypothesis	Population variances are equal.	Population variances are equal.	Population variances are equal.
	Result	Hypothesis is not rejected.	Hypothesis is not rejected.	Hypothesis is rejected.
t-test (Two-tailed)	p-value *	0.868	0.565	0.705
	Null hypothesis	Population means are equal.	Population means are equal.	Population means are equal.
	Result	Hypothesis is not rejected.	Hypothesis is not rejected.	Hypothesis is not rejected.

*Two t-tests, “t-test on two samples with equal variances” and “t-test on two samples with unequal variances” were used properly according to the results of the F-test.

Table 7 Information on records with the maximum and minimum absolute values of correlation coefficients

	Combination	Absolute value of correlation coefficient	KiK-net record name	Station name	Table 1 No.	Epicentral area	Figure number
Maximum	EW-NS	0.587	OKYH140010061330	HOKUBO	1	Western Tottori Pref.	Fig. 5 (a)
	NS-UD	0.413	KMMH161604142126	MASHIKI	14	Kumamoto, Kumamoto Pref.	Fig. 5 (b)
	UD-EW	0.368	GNMH131103120359	MINAKAMI2	11	Northern Nagano Pref.	Fig. 5 (c)
Minimum	EW-NS	0.001	IWTH250806140843	ICHINOSEKI -W	8	Southern inland, Iwate Pref.	Fig. 6 (a)
	NS-UD	0.001	YMNH111103152231	OHTSUKI	12	Eastern Shizuoka Pref.	Fig. 6 (b)
	UD-EW	0.004	KMMH061604142126	HAKUSUI	14	Kumamoto, Kumamoto Pref.	Fig. 6 (c)

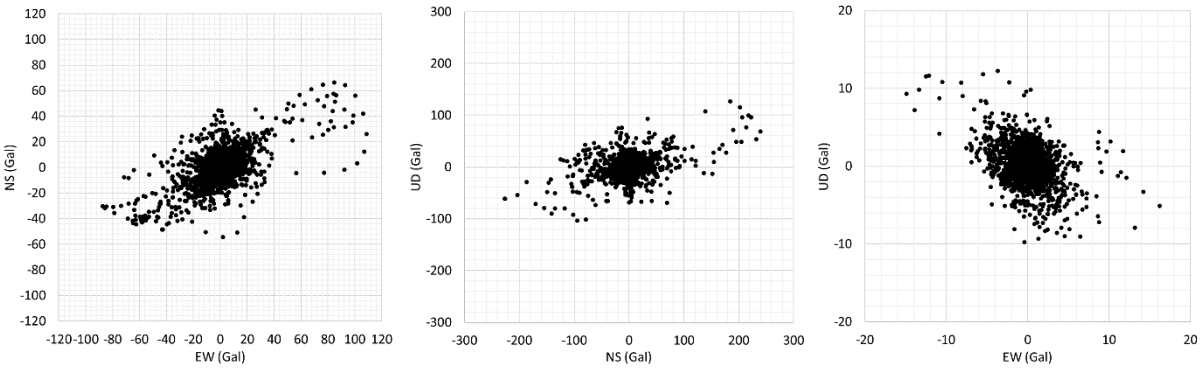

(a) EW-NS (b) NS-UD (c) UD-EW

Fig. 5 Acceleration records with the maximum absolute value of correlation coefficients

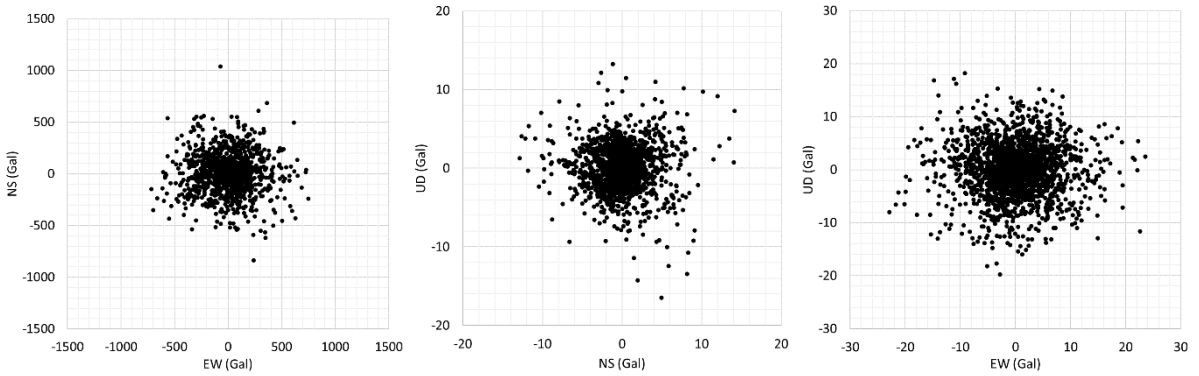

(a) EW-NS (b) NS-UD (c) UD-EW

Fig. 6 Acceleration records with the minimum absolute value of correlation coefficients

4.2 Effect of various parameters on correlation coefficients

In Chen[5], the correlation coefficients for a total of 129 acceleration records were calculated and statistically processed, but no analysis of the effects of various parameters, such as earthquake characteristics and underground geotechnical conditions at the observation stations, on the correlation coefficients was conducted. If correlation coefficients of actual ground motions depend on these parameters, they should be kept in mind when generating simulated ground motions. Therefore, we took earthquake magnitude (Mj), hypocentral depth, and hypocentral distance as indicators related to the earthquake, P-wave velocity (Vp) and S-wave velocity (Vs) of the ground where the seismograph was installed as indicators related to the observation station, and maximum acceleration (root-mean-square of three components) and the ratio of maximum acceleration of each component as indicators related to the size of record, then analyzed the effects of these indicators on the correlation coefficient. In addition, the difference in occurrence time of the maximum acceleration of each component (referred to as Δt in this paper)[18), 19)] was also selected as an indicator that may affect the correlation coefficient.

In the analysis, magnitude (M), hypocentral distance (X), and shear wave velocity (Vs) were selected as representative indicators of the earthquake source, propagation process and observation station, respectively. Then, each indicator was categorized into four groups according to its size, and statistical processing was performed of the correlation coefficient and the absolute value of the correlation coefficient. Stations for which Vs was not published were excluded from the analysis.

Table 8 shows the results of the statistical analysis. The means of the correlation coefficients were almost zero for all categories of the indicators. For M and X, the absolute values of the correlation

coefficients for each category were found not to be significantly different from each other. On the other hand, for Vs, the absolute value of the correlation coefficient tended to increase as Vs increased. This is because the absolute value of the correlation coefficients naturally tends to be larger as the variation of correlation coefficients increases (i.e., standard deviation of the correlation coefficients becomes larger).

Accordingly, the same F-tests as described in Section 4.1 were conducted for the correlation coefficients between adjacent categories. The results found that it cannot be said that there is a difference in the population variances for "Category c-1 and Category c-2" and "Category c-3 and Category c-4", while as for "Category c-2 and Category c-3", it was found that there is a difference in the population variances. As described, since the result does not indicate that "there are differences in the population variances" throughout the entire categories, it cannot be said at the current point in time that the relationship between each indicator and the absolute values of the correlation coefficients should be considered based on the categorization regarding Vs. To be sure, F-tests were also performed for the correlation coefficients between adjacent categories for magnitude M and hypocentral distance X. It was found that it cannot be said that there is a difference in the population variances between any of the categories.

Based on the above, when analyzing each indicator and absolute values of correlation coefficients, it was decided to analyze the overall trend without categorizing the representative indicators into smaller categories.

Table 8 Statistical analysis results when categorizing the representative indicators into four categories

Categorization method	Category	Number of data	Correlation coefficient		Absolute value of correlation coefficient
			Mean	Standard deviation	
(a) Categorizing magnitude into 4 groups	(a-1) M<6.0	30	−0.003	0.143	0.116
	(a-2) 6.0≦M<7.0	285	0.005	0.145	0.111
	(a-3) 7.0≦M<8.0	153	−0.016	0.142	0.110
	(a-4) 8.0≦M	30	−0.024	0.135	0.105
(b) Categorizing hypocentral distance into 4 groups (Unit: km)	(b-1) X<50	348	0.001	0.146	0.112
	(b-2) 50≦X<100	51	0.000	0.137	0.106
	(b-3) 100≦X<150	48	−0.033	0.132	0.108
	(b-4) 150≦X	24	−0.019	0.138	0.103
(c) Categorizing Vs into 4 groups (Unit: m/s)	(c-1) Vs<1000	135	0.005	0.116	0.090
	(c-2) 1000≦Vs <2000	189	−0.004	0.134	0.108
	(c-3) 2000≦Vs <3000	135	−0.018	0.167	0.129
	(c-4) 3000≦Vs	12	−0.065	0.240	0.192

Figures 7 through 10 show the relationship between four of the analyzed indicators (magnitude, hypocentral distance, Vs of the ground, and the absolute value of the difference in occurrence time of the maximum acceleration for each component) and the absolute value of the correlation coefficient. The categorization method (c) described above was adopted as an example, and each category was indicated by color coding. Figures 7 through 10 also show that there is no clear correlation between each indicator and the absolute value of the correlation coefficient in the analysis with any of the indicators. And this can be seen also from the fact that the coefficients of determination (R^2), assuming a linear regression, are in order 0.001, 0.001, 0.031 and 0.008, which are small. The same was basically true for the other indicators not shown in Figs. 7 through 10, and no correlation was found between each indicator and the absolute value of the correlation coefficient. In this study, the absolute values of the correlation coefficients were displayed following Chen[5], but no correlation was found either with each parameter in the analysis of correlation coefficients (without taking absolute value).

In the future, it is necessary to examine when the correlation coefficient of actual ground motions becomes large (or small). In particular, it is essential to examine the factors that cause the correlation coefficient to be large when the orbit of two components have a major axis direction, in combination with the relationship between the source characteristics and observation station, the propagation path,

the topographical and geological conditions at the observation station, and the characteristics of the underground geological/geotechnical structure.

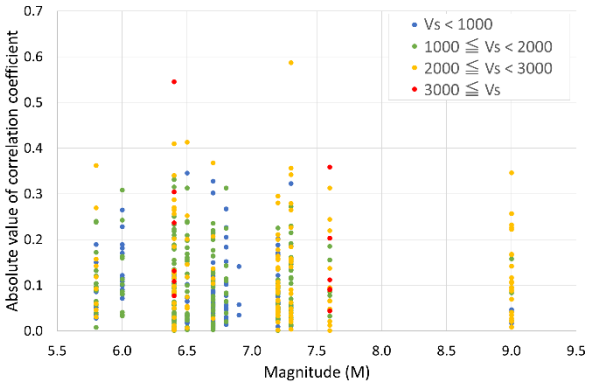

Fig. 7 Relationship between magnitude and absolute value of correlation coefficient

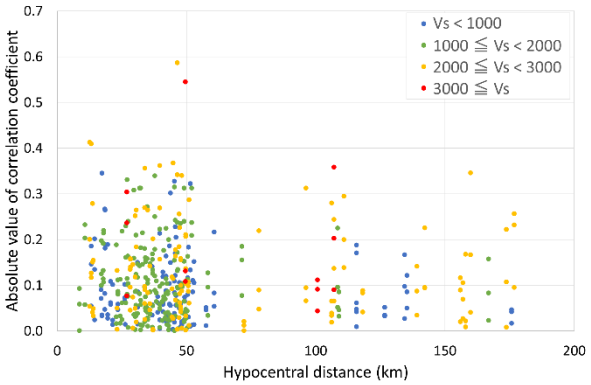

Fig. 8 Relationship between hypocentral distance and absolute value of correlation coefficient

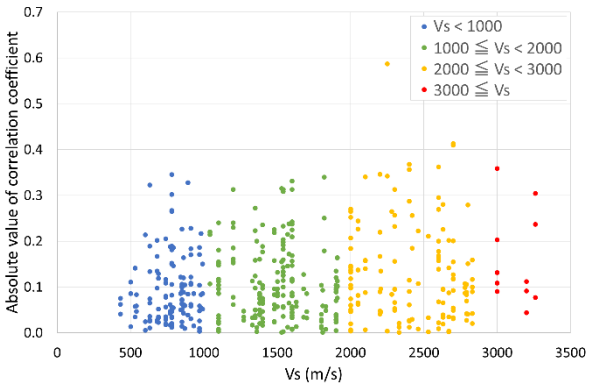

Fig. 9 Relationship between Vs of the ground and the absolute value of the correlation coefficient

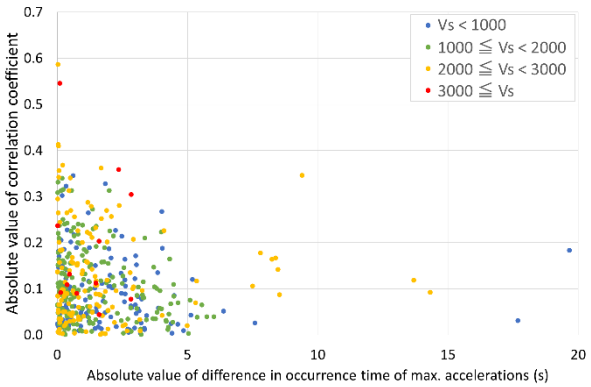

Fig. 10 Relationship between absolute value of Δt and absolute value of correlation coefficient

4.3 Effect that coordinate axes of orthogonal horizontal components have on the correlation coefficient

As can be seen from Eq. (2), since the correlation coefficient is not an invariant to the coordinate system, even for the same data set, the correlation coefficient will change depending on how the coordinate axes of the orthogonal horizontal components are taken. For example, the correlation coefficient would change if the orientation of one of the horizontal components of the earthquake ground motion at the observation station were to be rotated from geodetic north to Plant North, which is the north direction on the design drawing of the power plant. For this reason, since the correlation coefficient has an arbitrariness, it is necessary to discuss the effect on the correlation coefficient of how to establish the coordinate axes of the orthogonal horizontal components.

Therefore, we analyzed the correlation coefficients when the orthogonal horizontal coordinate axes (x- and y-axis) were rotated by 1 degree from 1 degree to 360 degrees (360 cases) for all cases of acceleration records for the above-mentioned 166 observation stations and conducted a statistical analysis. The specific procedure is as follows: first, the orientation is corrected based on the NIED observation station information, then the EW direction (x-axis) and NS direction (y-axis) are established. Next, the x-y coordinate axis is rotated in 1-degree increments, with counterclockwise as positive, to set

the x'-y' coordinate axes. Then, the correlation coefficient is calculated adopting the acceleration components in the x'-y' coordinate axes.

Figure 11 shows the analysis result for the maximum correlation coefficient (0.702) when rotated 360 degrees. This is the result of the analysis of the YMNH08 (Nishinohara) record for No. 12 (eastern Shizuoka Pref.) in Table 1. As can be seen from Fig. 11, the correlation coefficient between the EW (x component) and NS (y component) components varies sinusoidally with the rotation of the coordinate axes. On the other hand, the correlation coefficient between the NS component (y component) and the UD component (z component) as well as the correlation coefficient between the UD component (z component) and the EW component (x component) change in one cycle during a 360-degree rotation of the coordinate axes. The reason for these fluctuations is that the x-axis and y-axis are rotated, while the z-axis is generally adopted in the vertical direction, and since there is no arbitrariness here, no rotation of z-axis is necessary. Thus, since the correlation coefficient depends on the selected coordinate axes, it is considered necessary to confirm the validity of statistical processing results based on the observation records quantified using arbitrary coordinates (usually NS and EW).

Therefore, as described below, we decided to compare Analysis A with Analysis B. Analysis A: Analysis of 166 observation records without rotation of the coordinate axes as described in Sections 4.1 and 4.2. That is, the analysis for 498 (166 × 3) correlation coefficients for the NS and EW components, which are the original data. Analysis B: Analysis with 360-degree rotation. That is, an analysis for all 179,280 (166 × 3 × 360) correlation coefficients.

Table 9 shows the results of the statistical analysis for Analysis A and Analysis B. First, looking at the correlation coefficient, the mean of Analysis A is −0.005, while that of Analysis B is 0.000, almost the same. The standard deviation for Analysis A is 0.143, while that for Analysis B is 0.147, which is also almost the same. On the other hand, for the maximum and minimum, Analysis A is smaller than Analysis B. Here, the minimum value, which is negative, is compared in absolute value. Next, looking at the absolute values of the correlation coefficients, the mean of Analysis A is 0.111, while that of Analysis B is 0.112, almost the same. The maximum for Analysis B is 0.702 compared to 0.587 for Analysis A and Analysis B is clearly larger than Analysis A. The minimum value for Analysis B is 0.000 compared to 0.001 for Analysis A, which is almost the same.

The basic characteristics are shown in Table 9. Here, from the viewpoint of facilitating the contrast between Analysis A and Analysis B and the contrast with Chen[5)], the non-exceedance probability (cumulative probability) was analyzed using the absolute value of the correlation coefficient as an indicator. The results are shown in Fig. 12. It can be seen in Fig. 12 that the deviation between two curves of the non-exceedance probabilities of Analysis A and Analysis B is slight. Therefore, it can be said that, under the assumption that sufficient statistical data are available as in these analyses in this study, it is sufficient to analyze the correlation coefficients with the given coordinate axes. For reference, referring to Fig. 12 in terms of the "absolute value of correlation coefficient being 0.16 or less" which Chen[5)] and USNRC[4)] use as a criterion for simultaneous input ground motions, the non-exceedance probability is 0.767 for Analysis A, and it is 0.750 for Analysis B.

For acceleration records composed of two wave groups, it has already been mentioned in Section 3.2.2 that the first wave group is to be applied to perform the analysis of correlation coefficients etc. in this paper. The results of the analysis pertaining to the selection of the wave group are presented here for reference. Figure 13 shows the results of Analysis B for MYGH04 (Towa), also introduced in Section 3.2.2, and shows the correlation coefficients and the difference in occurrence time of the maximum acceleration for each component (referred to as Δt in this paper) for the EW component (x component) and NS component (y component). When the entire analysis section including the two wave groups is used as the analysis section for Δt, it can be seen that Δt (black dashed line) fluctuates significantly during a 360-degree rotation of the coordinate axes. This is due to the fact that the maximum of each component and its occurrence time varies with rotation of the coordinate axes, and that the maximum moves from the first wave group to the second wave group across a certain rotation angle. In contrast, no such phenomenon appears in Δt (red dashed line) when the first wave group is employed as the analysis section, and the fluctuation simply expresses the effect of rotation of the coordinate axes. In this paper, for the reasons discussed in Section 3.2.2, the correlation coefficient and Δt based on the first wave group are adopted in the analysis.

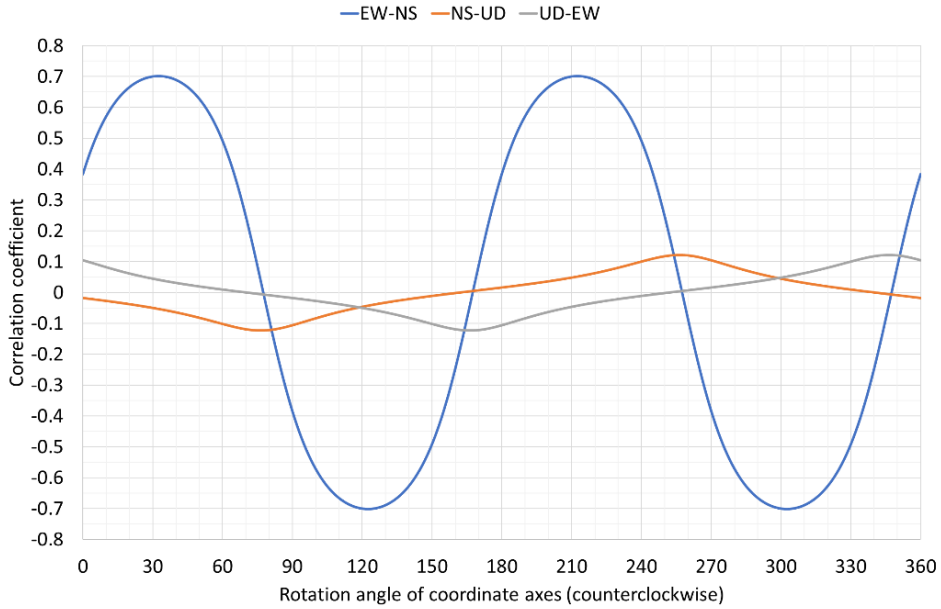

Fig. 11 Fluctuation of correlation coefficients when the coordinate axes are rotated (YMNH081103152231)

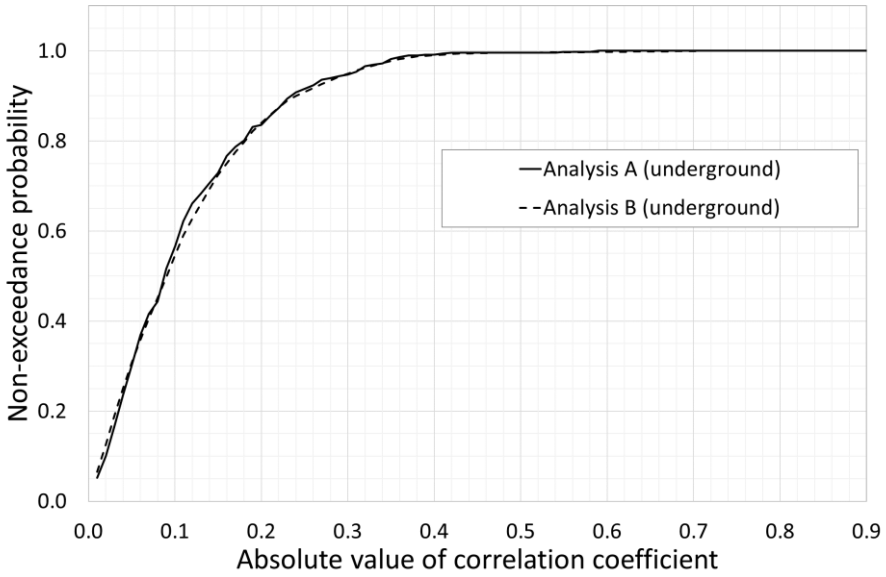

Fig. 12 Non-exceedance probability of absolute value of correlation coefficients

Table 9 Analysis results when the coordinate axes are rotated (KiK-net, underground)

	Correlation coefficient		Absolute value of correlation coefficient	
Analysis type	A	B	A	B
Number of data	166 × 3	166 × 3 × 360	166 × 3	166 × 3 × 360
Mean	−0.004	0.000	0.111	0.112
Standard deviation	0.143	0.147	–	–
Maximum	0.587	0.702	0.587	0.702
Minimum	−0.546	−0.702	0.001	0.000

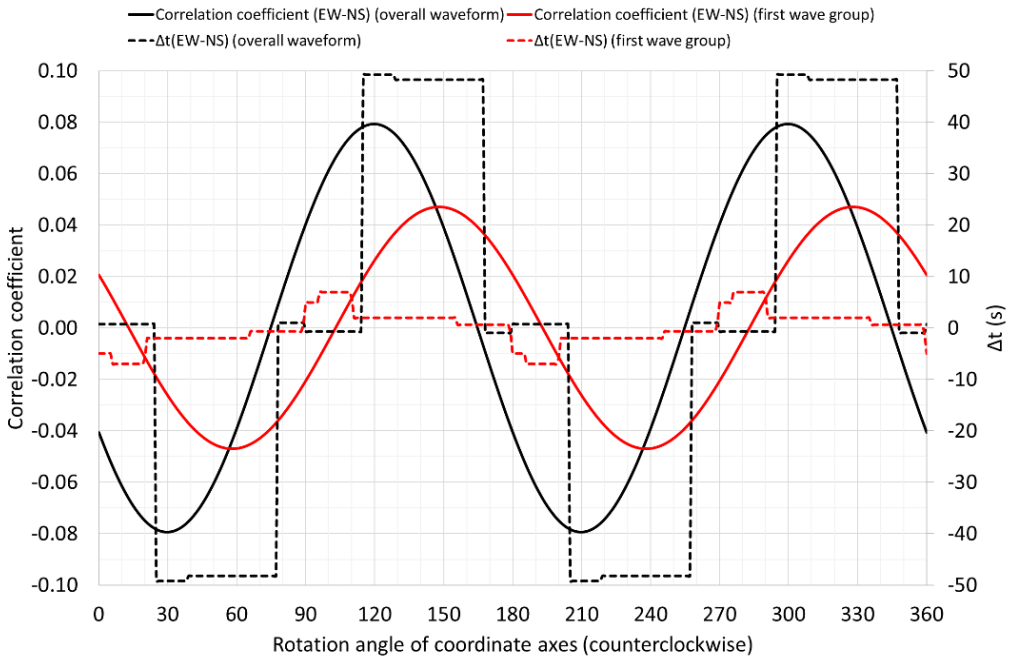

Fig. 13 Fluctuation of correlation coefficient and Δt when the coordinate axes are rotated (MYGH041103111446)

4.4 Comparison of underground and surface records

As mentioned earlier, this paper is based on an analysis of KiK-net subsurface records, since the design basis earthquake ground motions of nuclear facilities are defined at the free rock surface. However, it is important to understand the relationship between the correlation coefficients of underground records and those of surface records, in addition to that, there is a possibility of obtaining useful information for future design. Therefore, the same analyses were conducted for the surface records as for the underground records.

First, Analysis A was conducted for the surface records as a fundamental study. The results are shown in Fig. 14 in contrast to Analysis A for the underground records. Initially, we expected that there would be some correlation between the correlation coefficient in the underground and that on the surface, however Fig. 14 shows that there is no correlation between the two. This is true even when considering the absolute value of the correlation coefficient. Therefore, at the present stage, when considering the correlation coefficient of input ground motions, it can be said that it is sufficient to proceed on the assumption that there is no correlation between the underground and the surface. However, since the surface records during strong-motion earthquakes that are the subject of this study may be affected by nonlinearity of the ground, the relationship between the surface and underground correlation coefficients is a task for future study.

Table 10 Analysis results of the surface records (KiK-net, surface)

	Correlation coefficient		Absolute value of correlation coefficient	
Analysis type	A	B	A	B
Number of data	166 × 3	166 × 3 × 360	166 × 3	166 × 3 × 360
Mean	0.003	0.000	0.130	0.134
Standard deviation	0.173	0.177	–	–
Maximum	0.593	0.656	0.656	0.656
Minimum	−0.656	−0.656	0.000	0.000

Next, the same analyses for the underground records shown in Table 9 and Fig. 12 were performed for the surface records, and the results are shown in Table 10 and Fig. 16, respectively. The relationship between Analysis A and Analysis B for the surface records is the same as that described for the underground records in Section 4.3. Since the difference between the curves of the non-exceedance probabilities of Analysis A and Analysis B is slight, it can be said that the correlation coefficient should be analyzed in the given coordinate axes in the case that sufficient statistical data are available.

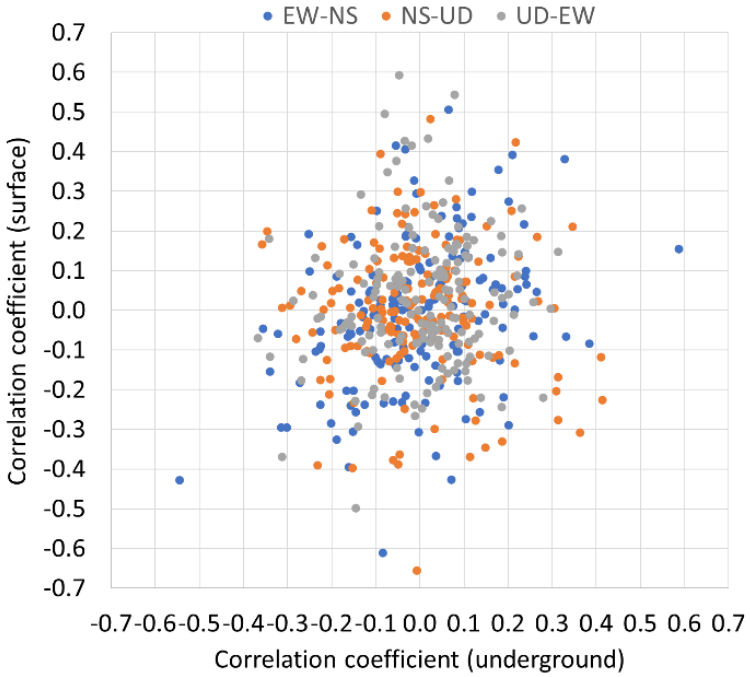

Fig. 14 Comparison between underground and surface with respect to correlation coefficient

4.5 Analysis results of outcropped bedrock records

As described in Section 2.2, 19 records from RK-net of the Central Research Institute of Electric Power Industry (CRIEPI) as shown in Table 2 were analyzed for the purpose of comparing the correlation coefficients between outcropped rock records and underground bedrock records. The procedure for analysis was as described in Section 3.2.1, and Analysis A and Analysis B were conducted in the same manner as for the KiK-net records. The results are shown in Table 11, along with the results of the analysis of the underground rock records (repost of Table 9). The results of Analysis A, the fundamental study, are shown in Fig. 15 in contrast to the results of the underground rock records (reproduction of Fig. 9). The number of outcropped bedrock records is 19, which is relatively small compared to the underground bedrock records, so it cannot be said definitively, but the standard deviation and the maximum of the correlation coefficients tend to be larger for the outcropped bedrock records.

Next, as in the previous sections, Fig. 16 shows the results of the analysis of the probability of non-exceedance for the absolute value of the correlation coefficients. For RK-net, unlike in the previous cases, since the deviation between two curves of the non-exceedance probabilities of Analysis A and Analysis B is observed, the number of statistical data may not be sufficient. In comparison with underground and surface records of KiK-net, non-exceedance probability of RK-net is close to that of KiK-net surface records. It should be noted that since the number of statistical data may not be sufficient as mentioned above, it is desirable to make a decision based on further accumulation of data in the future.

Table 11 Comparison of outcropped bedrock and underground bedrock

	Correlation coefficient				Absolute value of correlation coefficient			
Record type	Outcropped（RK-net）		Underground（KiK-net）		Outcropped（RK-net）		Underground（KiK-net）	
Analysis type	A	B	A	B	A	B	A	B
Number of data	19 × 3	19 × 3 × 360	166 × 3	166 × 3 × 360	19 × 3	19 × 3 × 360	166 × 3	166 × 3 × 360
Mean	−0.035	0.000	−0.004	0.000	0.142	0.142	0.111	0.112
Standard deviation	0.177	0.190	0.143	0.147	–	–	–	–
Maximum	0.379	0.814	0.587	0.702	0.618	0.814	0.587	0.702
Minimum	−0.618	−0.814	−0.546	−0.702	0.005	0.000	0.001	0.000

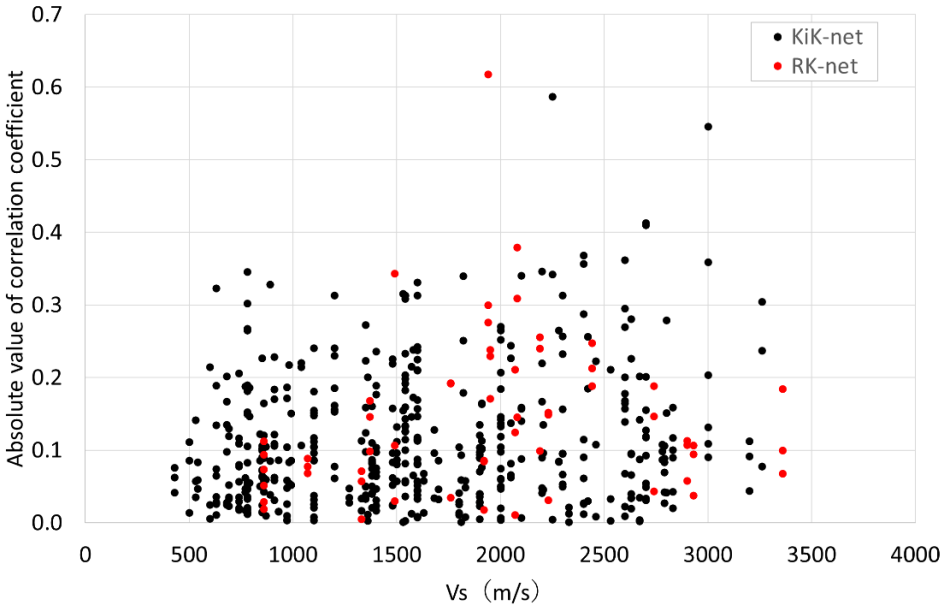

Fig. 15 Relationship between Vs and absolute value of correlation coefficient

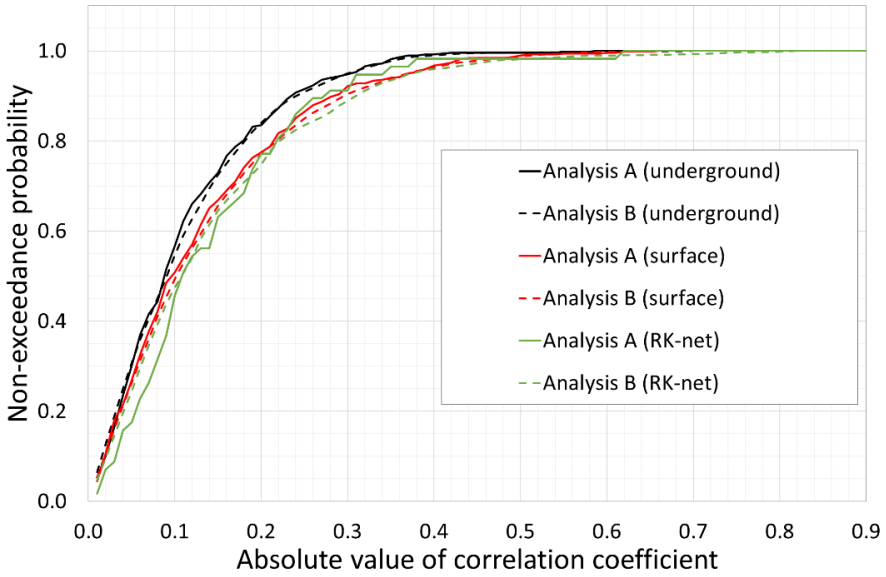

Fig. 16 Comparison of absolute non-exceedance probabilities of correlation coefficients

5. ANALYSIS RESULTS OF SIMULATED GROUND MOTIONS

5.1 Analysis results of correlation coefficient and absolute value of correlation coefficient

Simulated ground motions were generated using the method described in Section 2.3. An example of the 100 sets of simulated ground motions is shown in Fig. 17. In this example, the maximum accelerations are 468.0 Gal, 468.5 Gal, and 295.0 Gal for the EW, NE and UD components, in that order. The acceleration response spectra of the simulated ground motions illustrated in Fig. 17 is shown in Fig. 18 and the simulated ground motions are generally generated as per the target spectra.

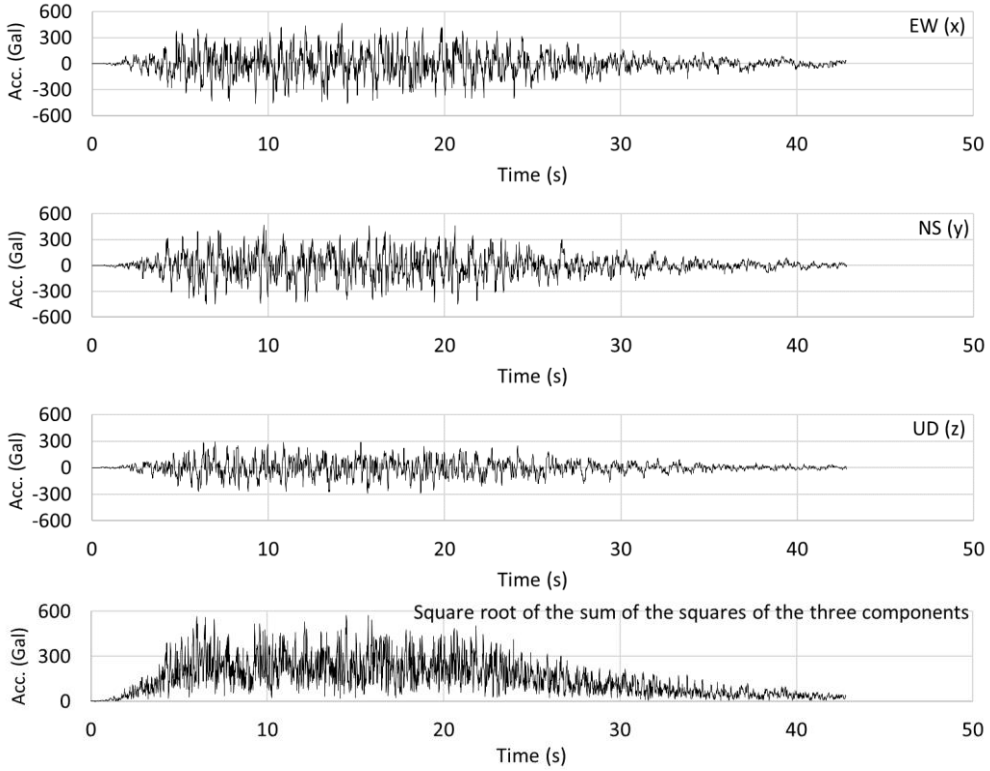

Fig. 17 Example of time-history waveform of simulated ground motion

The analysis of correlation coefficients was conducted in accordance with the procedure described in Section 3.2.1. However, simulated ground motion does not have a portion corresponding to a foreshock and aftershock unlike actual ground motion, and it is possible to establish the adopted section without visual confirmation. Therefore, steps 2 through 4 were conducted without setting the search section of step 1. The results of the analysis of the correlation coefficients for the simulated ground motions shown in Fig. 17 are shown in Table 12. It can be seen that the difference in the analysis section has little effect on the correlation coefficient.

Table 12 Effect of analysis section on correlation coefficient (simulated ground motion)

Analysis section	EW-NS (x-y)	NS-UD (y-z)	UD-EW (z-x)
case (1) 0–42.79 s (all data)	−0.03348	−0.08193	−0.01567
case (2) Not implemented	–	–	–
case (3) 0.63–42.79 s (adopted section)	−0.03348	−0.08193	−0.01568

A histogram of the absolute values of the correlation coefficients for the simulated ground motions is shown in Fig. 19. In addition to Analysis A, Analysis B was also conducted for the simulated ground

motions as well as the analyses performed for the actual ground motions. The results of the statistical analysis of Analysis A and Analysis B are shown in Table 13. And, as with the results of the analysis of actual ground motions described in Section 4.3, there is no significant difference between Analysis A and Analysis B in terms of the mean and standard deviation of the correlation coefficients and the mean of the absolute value of the correlation coefficients.

Next, Fig. 20 shows the non-exceedance probability (cumulative probability) of the absolute values of the correlation coefficients obtained using simulated ground motions. It is thought that Fig. 20 clarifies the characteristics of the correlation coefficients of the simulated ground motions.

For the simulated ground motions, referring to Fig. 20 from the viewpoint of the "absolute value of correlation coefficient being 0.16 or less" following Chen[5] and USNRC[4], the non-exceedance probability for Analysis A is 0.967, while for Analysis B it is 0.982. Since Analysis B is not conducted in the process of generating simulated ground motions in general, we decided to look at the value of Analysis A. If 0.16 is employed as the criterion, 96.7% of the simulated ground motions meet the criterion.

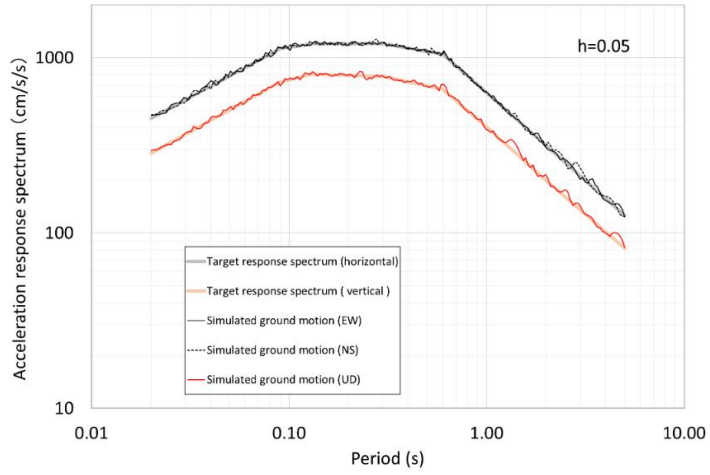

Fig. 18 Acceleration response spectra of simulated ground motions

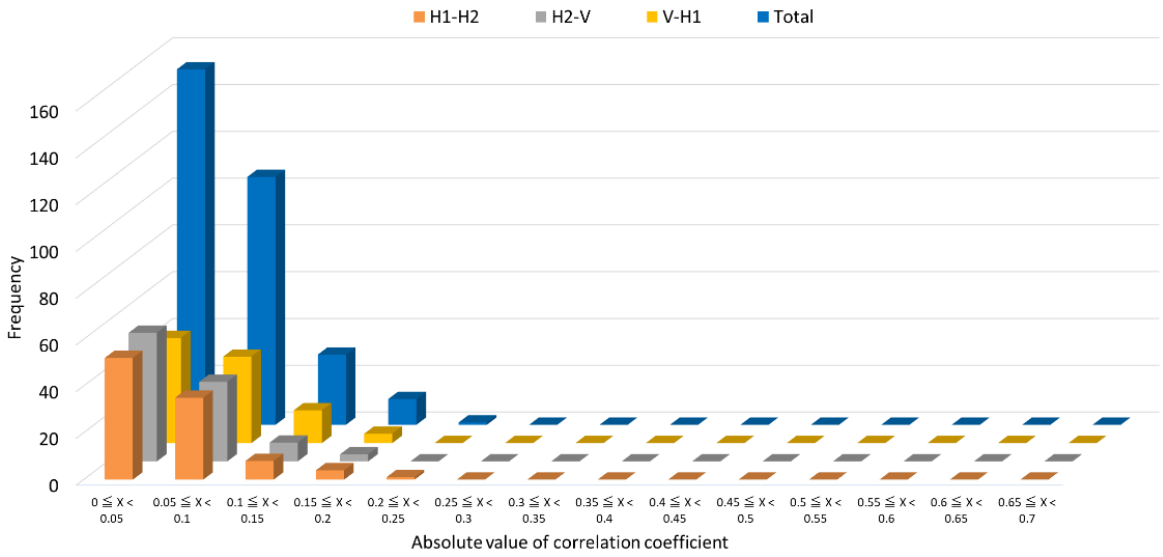

Fig. 19 Histogram of absolute values of correlation coefficients for simulated ground motions

Table 13 Analysis results of simulated ground motions

	Correlation coefficient		Absolute value of correlation coefficient	
Analysis type	A	B	A	B
Number of data	100 × 3	100 × 3 × 360	100 × 3	100 × 3 × 360
Mean	−0.003	0.000	0.057	0.051
Standard deviation	0.070	0.065	–	–
Maximum	0.182	0.232	0.210	0.232
Minimum	−0.210	−0.232	0.000	0.000

5.2 Discussion of the effect of various parameters on the correlation coefficient

For the simulated ground motions, the following parameters were also analyzed for their effects on the correlation coefficient. The parameters are as follows: maximum acceleration (root-mean-square of the three components), maximum acceleration (root-mean-square of the two components), ratio of the maximum accelerations of each component, and the difference in occurrence time of the maximum accelerations of each component. As a representative example, the relationship between the maximum acceleration (the square root of the sum of squares of the two components) and the absolute value of the correlation coefficient is shown in Fig. 21. There is no correlation between the two. In other words, there is no tendency that the absolute value of the correlation coefficient increases as the maximum acceleration of the simulated ground motion, which was generated to satisfy a certain criterion, increases.

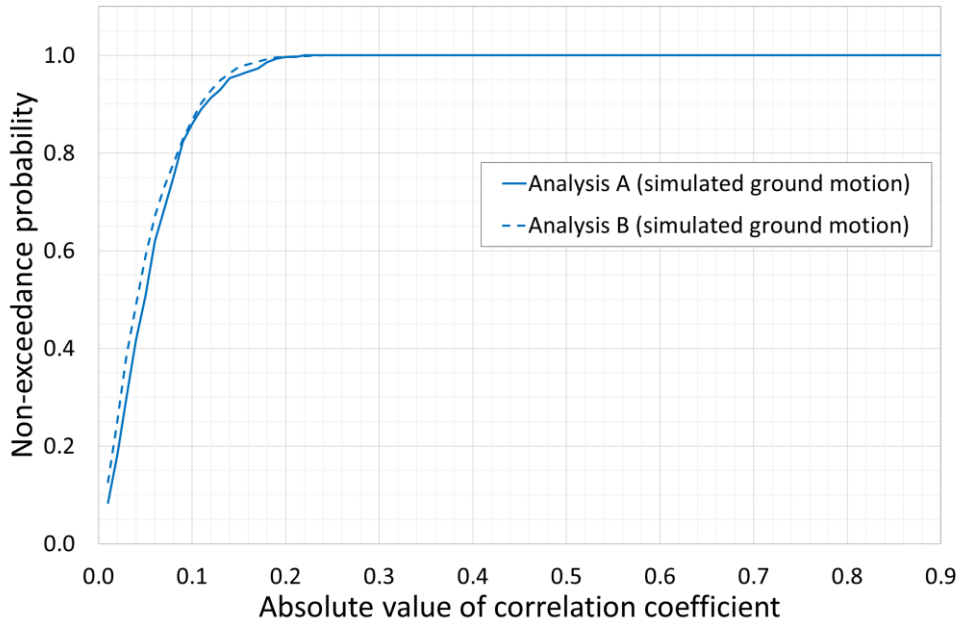

Fig. 20 Non-exceedance probability of the absolute value of the correlation coefficient for the simulated ground motions

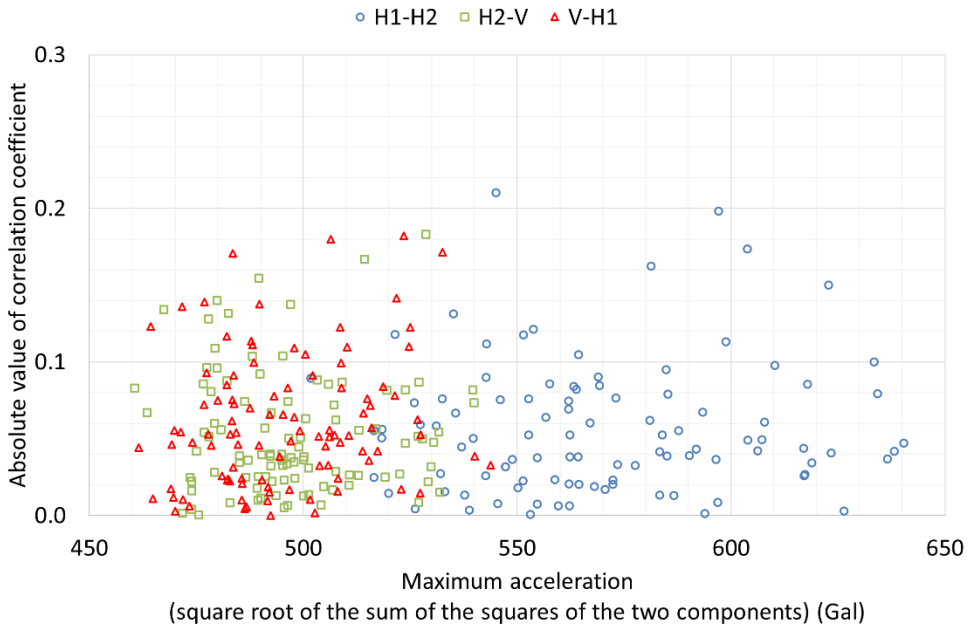

Fig. 21 Relationship between the maximum acceleration of the simulated ground motions and the absolute value of the correlation coefficient

6. RELATIONSHIP BETWEEN ELLIPTICAL COMPONENT OF POLARIZATION AND CORRELATION COEFFICIENT

Igarashi et al.[8] and Inoue et al.[9] proposed the utilization of the elliptical component of polarization (P_E) by Vidale[7] for evaluation when generating the seismic ground motion in two directions based on response spectrum, for the purpose of generating the time-history waveform in which the orbit of the two horizontal components is on a circle. The elliptical component of polarization P_E by Vidale[7] is determined to be an indicator to evaluate planarly or spatially the behavior of a particle due to seismic motion, with $P_E = 0$ corresponding to a linear orbit and $P_E = 1$ corresponding to a circular orbit. Therefore, the correlation coefficient, which is the subject of this study, is qualitatively inversely related to P_E in terms of the change in values corresponding to the orbit. However, they are considered to be useful indicators in terms of evaluating the relationship between the two orthogonal components of actual ground motions and/or simulated ground motions.

Accordingly, in this chapter, the two horizontal components of the 166 actual ground motions and 100 combinations of simulated ground motions shown in Chapters 4 and 5 are considered. P_Es were obtained for the analysis section for which correlation coefficients were obtained and the relationship between P_Es and correlation coefficients was discussed. Here, for evaluation by P_E, as in Inoue et al.[9], the time history of P_E was analyzed and employed the indicator μ_a, which is obtained by averaging the weighted integrals of P_E based on the acceleration of the vector sum of two components at each time (weighted average of P_E with respect to acceleration). The reason why μ_a was adopted as a subject for comparison of the correlation coefficient is that Inoue et al.[9] also adopted μ_a as a representative value of seismic motion records in their discussion.

A comparison between the maximum of the correlation coefficients (without taking absolute value), which was obtained from Analysis B in Section 4.3, and μ_a is shown in Fig. 22 and Fig. 23. The reason for adopting the maximum value of Analysis B here is as follows. P_E, the original data of μ_a used by Inoue et al. [9], is an indicator that quantifies the orbit of two-dimensional particle motion in the x-y plane, and since eigenvalue analysis is performed when P_E is obtained, μ_a is a value that is invariant to the coordinate system in this sense. In contrast, since the correlation coefficient depends on the Cartesian coordinate system employed arbitrarily, it is considered appropriate to adopt the maximum for the 360-

degree rotation case (Analysis B).

For actual ground motions, Fig. 22 shows overall that there is an inversely proportional relationship inferred from the definitions of the two indicators. On the other hand, it is characteristic that the distribution ranges of the two indicators in Fig. 22 are very different from each other, even though both indicators can take values between 0 and 1. While the correlation coefficient is generally distributed in the range of 0 to 0.7, the μ_a obtained from P_E is generally distributed in the range of 0.2 to 0.36, which is much narrower than the correlation coefficient, with many data concentrated in the range of 0.3 to 0.32. This trend is also true for the simulated ground motions shown in Fig. 23. That is, the correlation coefficient is generally distributed in the range of 0 to 0.2, while the μ_a is distributed in the range of 0.3 to 0.35, which is generally similar to the range where the μ_a was concentrated for the actual ground motions. In addition, the expected inversely proportional relationship between the two indicators is not observed. According to Inoue et al.[9], μ_a, i.e., P_E weighted by the acceleration of the vector sum of two components, was evaluated for several actual ground motions and was reported to be around 0.3 regardless of whether they were subduction-zone earthquakes or inland earthquakes, and the value of μ_a in this study is in harmony with this result.

From these results, it can be said that the correlation coefficient has a relatively wider distribution range than μ_a and may be more appropriate as a more detailed (with higher resolution) indicator of the characteristics between the two orthogonal components of ground motions.

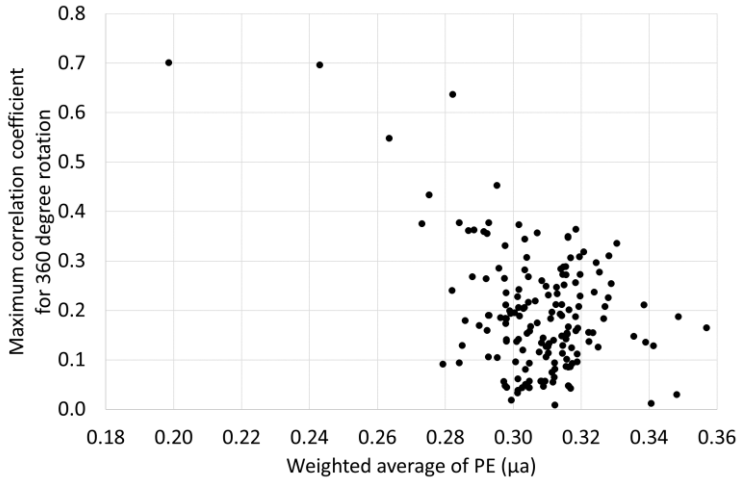

Fig. 22 Relationship between correlation coefficient of actual ground motion and μ_a

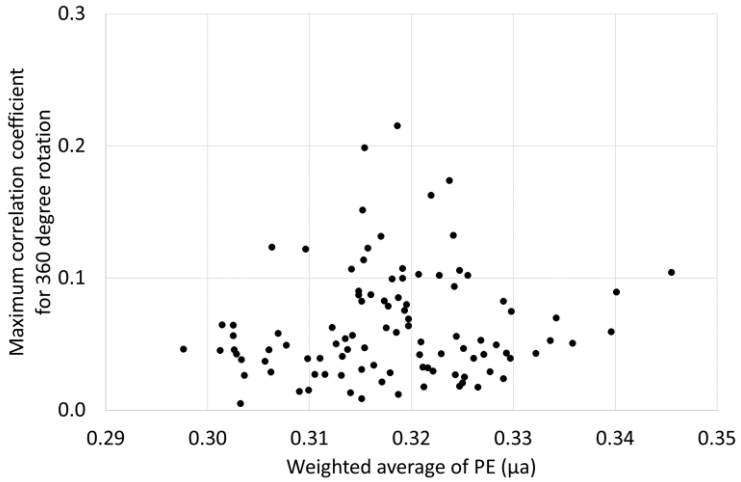

Fig. 23 Relationship between correlation coefficient of simulated ground motions and μ_a

7. CONCLUSIONS

In this paper, we analyze the correlation coefficients by Chen[5] using the strong-motion records of a total of 166 points (accumulated number) on KiK-net of NIED for earthquakes with seismic intensity of "6 Upper" and "7" since 2000 in Japan, and also analyzed the relationship between various parameters related to earthquakes and correlation coefficients or absolute values of correlation coefficients used by USNRC[4] and others. In addition, we analyzed the correlation coefficients of the simulated ground motions with a method widely adopted in practice today. As a result, the following conclusions were obtained.

- The mean of the correlation coefficients, without taking absolute values of actual ground motions at a total of 166 stations (accumulated number) in Japan, was −0.004 with standard deviation of 0.143, while the mean of the absolute value of correlation coefficient was 0.111. These values are not significantly different from those of Chen[5], a previous study.
- The mean of the correlation coefficients, without taking absolute values of 100 simulated three-component ground motions generated by a method based on a general response spectrum with phase angles given by uniformly distributed random number, was −0.003 with standard deviation of 0.070, while the mean of the absolute value of correlation coefficient was 0.057.
- As stated above, the correlation coefficients without taking absolute values generally follow a normal distribution with the mean, which is set to 0, for both actual and simulated ground motions. On the other hand, almost all of the three-component simulated ground motions based on the general method satisfy the criteria, stipulated by the USNRC[4], for absolute values of correlation coefficients based on Chen[5].
- No correlation was found between each of the following indicators and the correlation coefficient or the absolute value of the correlation coefficient for the observation records under consideration. The indicators are as follows: earthquake magnitude, hypocentral depth, hypocentral distance, Vp and Vs of the ground, maximum acceleration, ratio of maximum acceleration of each component, and the difference of occurrence time of the maximum acceleration of each component.
- No correlation was found between each of the following indicators and the correlation coefficient or the absolute value of the correlation coefficient for the simulated ground motions as well. The indicators are as follows: the maximum acceleration, the ratio of the maximum acceleration of each component, and the difference in occurrence time of the maximum acceleration of each component.
- Observation records of the two horizontal components are provided as components in the NS and EW directions in which seismometers are typically installed. And, the correlation coefficient fluctuates depending on how to establish the coordinate axes for the orthogonal horizontal components in the analysis. Therefore, it is important to understand the amplitude of the fluctuation in order to comprehend the correlation coefficient of the record itself. However, when statistical processing of correlation coefficients is performed with more than a certain number of statistics (166 in this study), it is possible to discuss the results of analysis with data in the given coordinate axes, for example, in the NS and EW directions, since the selection of the coordinate axes have almost no effect.
- No correlation was found between the correlation coefficients of the underground record and the correlation coefficients of the surface record at the vertical array observation stations (KiK-net). The same was true for the absolute values of the correlation coefficients. However, since the records used in this study were obtained during strong-motion earthquakes, the relationship between the surface and underground correlation coefficients is an issue for future study, since the surface records are considered to be affected by nonlinearities of the ground.
- The absolute value of the correlation coefficient for the outcropped bedrock record (RK-net), which is the so-called 2E waves, tends to be larger than that for the underground bedrock record (KiK-net, underground), which is the so-called E + F waves. However, since the number of RK-net data is smaller than that of KiK-net data, more data needs to be accumulated in the future.
- From the viewpoint of evaluating the relationship between the two components of actual ground motion and simulated seismic motion, the elliptical component of polarization P_E (P_E with the

acceleration of the vector sum of two components as a weight), which is an indicator to evaluate planarly or spatially the behavior of the particle due to seismic motion, was compared to the correlation coefficient. As a result, for the actual observation records, overall, an inversely proportional relationship was observed between the changes of both indicators. On the other hand, it was found that the correlation coefficient may be a relatively more detailed and a higher resolution measure of the characteristics between the two orthogonal components of the earthquake ground motion, since the correlation coefficient has a larger range of variation than the P_E for the same data set.

- A series of statistical analyses have enabled us to comprehend the characteristics of the correlation coefficients of actual strong ground motions. Therefore, it can be said that the result of this study from an engineering point of view is that a guideline for the value of the correlation coefficient, which should be equipped by the simulated ground motions in the future seismic design, was obtained.

Finally, we discuss future tasks. In this paper, by analyzing the correlation coefficients of actual and simulated ground motions, we were able to comprehend the fundamental characteristics such as the distribution of correlation coefficients and statistical quantities based on them, the relationship between the coordinate axes of orthogonal horizontal components and the relationship between the simulated ground motions generated adopting the method widely used in current practice and actual ground motions in terms of the correlation coefficient. However, it is necessary to examine in what cases the correlation coefficients of actual ground motions become large (or small), especially in the case that the orbit of the two components with large correlation coefficient has a major axis direction, along with the relationship between the source characteristics and observation stations, the topographical and geological conditions at the observation stations along the propagation path, and the characteristics of underground geological/geotechnical structures as well. We will continue to study this task and make use of this information in seismic design.

ACKNOWLEDGMENT

In this study, we utilized the “Seismic Intensity Database Search” of the Japan Meteorological Agency (JMA) to select the earthquakes to be studied. We also utilized the KiK-net observation records of the National Research Institute for Earth Science and Disaster Resilience (NIED) and the RK-net observation records of the Central Research Institute of Electric Power Industry (CRIEPI) as earthquake ground motion records for analysis. We thank Mr. Eiji Shirai (former ATENA employee) for his valuable comments in preparing the paper. Finally, we would like to express our gratitude to all the people involved.

APPENDIX: RELATIONSHIP BETWEEN VALUE OF CORRELATION COEFFICIENT AND PLANAR DISTRIBUTION OF TWO ACCELERATION COMPONENTS

The purpose of this appendix is to enhance understanding of the correlation coefficient of the two acceleration components by showing clearly how the planar distribution of those two components changes as the value of the correlation coefficient of the two acceleration components changes.

Among the 100 pairs of simulated ground motions described in Sections 2.3 and 5.1 of the main text, we selected one combination with a correlation coefficient of near zero for the two horizontal ground motions and applied it to this examination. The time-history waveforms of the two selected combination of horizontal ground motions are shown in Fig. A1, and the acceleration distribution on the EW-NS(x-y) plane is shown in Fig. A2. The correlation coefficient between the two horizontal ground motions analyzed based on Eq. (2) in the main text is −0.002. Figure A2 shows that this pair of ground motions vibrates uniformly in all directions. In addition, the standard deviations of the two ground motions are 124.9 Gal and 124.2 Gal, respectively.

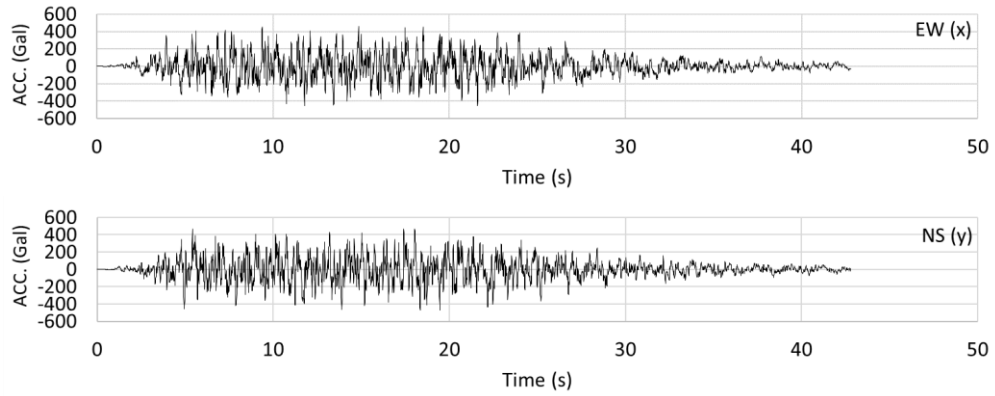

Fig. A1 Example of simulated ground motions with a correlation coefficient of near zero for two horizontal ground motions

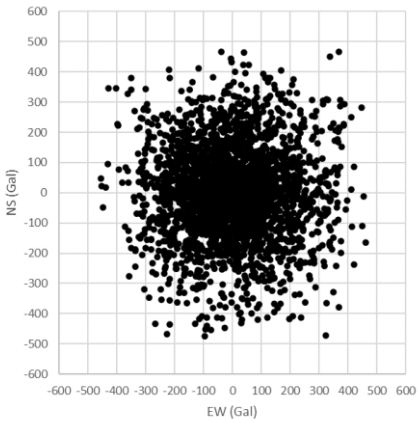

Fig. A2 Acceleration distribution on EW-NS(x-y) plane

The x- and y-component of the two aforementioned ground motions were taken as variables X and Y, respectively, and variable Z was generated based on Eq. (A1), in which ρ is the correlation coefficient between variable X and variable Z. However, for Eq. (A1) to hold, variables X and Y must be independent and their respective standard deviations must be the same. In contrast, as mentioned above, the selected ground motions almost satisfy these conditions.

$$Z = \rho X + \sqrt{1-\rho^2}Y \tag{A1}$$

Figure A3 shows the acceleration distribution on the EW-NS (x-y) plane, with the variable Z generated according to Eq. (A1) as the new NS component (y component) and the variable X substituted into Eq. (A1) as the EW component (x component). It is understood from Fig. A3 that a seismic ground motion with large correlation coefficient is the ground motion that moves in a certain direction, while that with small correlation coefficient is the motion that vibrates uniformly in all directions.

In the case of ρ = 1.0 in Fig. A3 (f), the acceleration distributions are shown in Fig. A4 (a), (b) and (c) when all of the time-history waveform of the NS component (y component) in the figure is multiplied by a factor of 0.8, 0.6, or 0.4. As is clear from Eq. (2) in the main text, multiplying one of the two components by a certain multiplying factor does not change the correlation coefficient. Therefore, the correlation coefficients for the three cases shown in Fig. A4 are all 1.0, the same as in Fig. A3(f). In other words, seismic ground motions with a correlation coefficient of 1.0 are those that move in a certain direction and not necessarily in the direction of 45 degrees (in the direction of x = y in the case of x-y space).

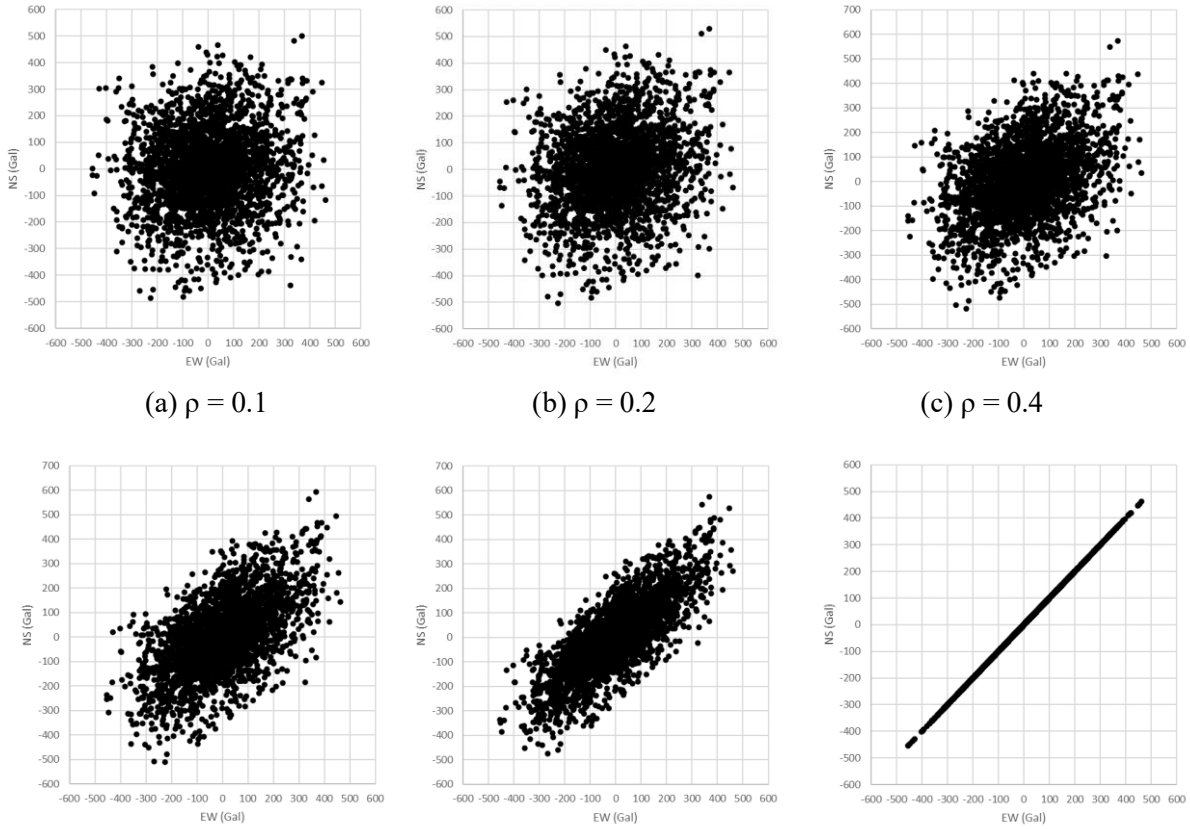

(a) ρ = 0.1 (b) ρ = 0.2 (c) ρ = 0.4

(d) ρ = 0.6 (e) ρ = 0.8 (f) ρ = 1.0

Fig. A3 Relationship between the value of the correlation coefficient and the planar distribution of the two acceleration components

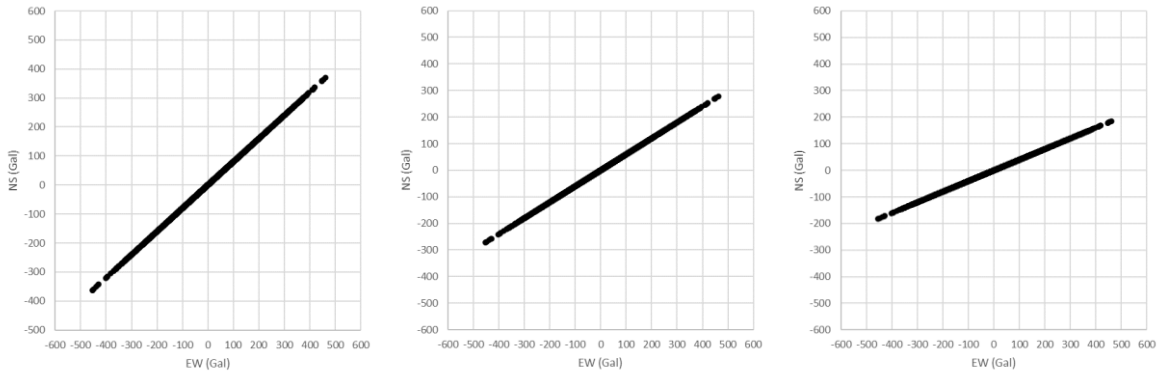

(a) MF = 0.8 (b) MF = 0.6 (c) MF = 0.4

Fig. A4 Variation of the planar distribution of the two acceleration components when the NS component is multiplied by the multiplying factor (MF).

REFERENCES

1) The Japan Electric Association: Technical Guidelines for Seismic Design of Nuclear Power Plant, JEAG4601-2015, pp. 31–37, 2015 (in Japanese).
2) Noda, S., Yashiro, K., Takahashi, K., Takemura, M., Ohno, S., Tohdo, M. and Watanabe, T.: Response Spectra for Design Purpose of Stiff Structures on Rock Sites, *OECD-NEA Workshop on the Relations between Seismological DATA and Seismic Engineering*, Istanbul, pp. 399–408, October 16–18, 2002.
3) Earthquake Research Committee, Headquarters for Earthquake Research Promotion: Strong Ground Motion Prediction Method for Earthquakes with Specified Source Faults ("Recipe"), 2020 (in Japanese). https://www.jishin.go.jp/main/chousa/20_yosokuchizu/recipe.pdf (last accessed on Janyary 30, 2023)
4) United States Nuclear Regulatory Commission: Regulatory Guide 1.92 Revision 3 Combining Model Responses and Spatial Components in Seismic Response Analysis, 2012.
5) Chen, C.: Definition of Statistically Independent Time Histories, *Journal of the Structural Division*, Vol. 101, No. ST2, ASCE, pp. 49–51, 1975.
6) Atomic Energy Association: ATENA 20-NE01(Rev.0) Guidelines for the Design of Seismically Isolated Structures for Severe Accident Measures Facilities, 2020 (in Japanese).
7) Vidale, J. E.: Complex Polarization Analysis of Particle Motion, *Bulletin of the Seismological Society of America*, Vol. 76, No. 5, pp. 1393–1405, 1986.
8) Igarashi, A., Inoue, K., Furukawa, A., Uno, A. and Matsuda, H.: Synthesis of Bi-Directional Seismic Ground Motion by Standard and Complementary Waves for Seismic Design of Bridges, *Proceedings of the Japan Society of Civil Engineers (A1 Structural Engineering/Earthquake Engineering)*, Vol. 68, No. 4, pp. I_458–I_469, 2012 (in Japanese).
9) Inoue, K., Watanabe, K., Igarashi, A. and Hata, A.: Horizontal Plane Characteristics of Observed Strong Ground Motions and Generation of Bi-Axial Response Spectrum Compatible Bi-Directional Seismic Accelerograms, *Proceedings of the Japan Society of Civil Engineers (A1 Structural Engineering/Earthquake Engineering)*, Vol. 74, pp. I_555–I_568, 2016 (in Japanese).
10) National Research Institute for Earth Science and Disaster Resilience: *NIED K-NET, KiK-net*, 2019. https://www.doi.org/10.17598/NIED.0004
11) Shiba, Y. and Sato. H.: Series "New; Latest Information on Strong-Motion Observation" (No.13) Strong-Motion Observation System on Outcropped Rock (RK-net), Central Research Institute of Electric Power Industry, *Seismological Society of Japan Newsletter*, Vol. 73, No. NL5, pp. NL-5-17–NL-5-19, 2021 (in Japanese).
12) Kato, K., Miyakoshi, K., Takemura, M., Inoue, D., Ueta, K. and Dan, K.: Earthquake Ground Motions by Blind Faults in the Upper Crust—Categorization of Earthquakes Based on Geological Survey and Examination of the Upper Level from Strong Motion Records—, *Journal of Japan Association for Earthquake Engineering*, Vol. 4, No. 4, pp. 46–86, 2004 (in Japanese).
13) National Research Institute for Earth Science and Disaster Resilience Strong-Motion Seismograph Networks (K-NET, KiK-net). https://www.kyoshin.bosai.go.jp/ (last accessed on Januay 30, 2023)
14) Housner, G. W.: Intensity of Ground Shaking Near the Causative Fault, *Proceedings of the 3rd World Conference on Earthquake Engineering*, New Zealand, 3, pp. 94–109, 1965.
15) Bolt, B. A.: Duration of Strong Ground Motion, *Proceedings of the 5th World Conference on Earthquake Engineering, Rome*, 6-D, 292, 1973.
16) Trifunac, M. D. and Brady, A. G.: A Study on the Duration of Strong Earthquake Ground Motion, *Bulletin of the Seismological Society of America*, Vol. 65, No. 3, pp. 581–626, 1975.
17) Asano, K. and Iwata, T.: Source Model for Strong Ground Motion Generation in the Frequency Range 0.1–10 Hz during the 2011 Tohoku Earthquake, *Earth, Planets and Space*, Vol. 64, pp. 1111–1123, 2012. https://doi.org/10.5047/eps.2012.05.003
18) Sato. H. and Shiba, Y.: Estimation for the Time Lag of Maximum Acceleration between Vertical and Horizontal Ground Motion on Outcrop Rock Site, Architectural Institute of Japan, *Summaries of Technical Papers of Annual Meeting*, 21106, pp. 211–212, 2000 (in Japanese).
19) Yabana, S. and Ishida, K.: Evaluation of Vertical and Horizontal Seismic Loads—Effect of Fault

Mechanism and Vertical and Horizontal Seismic Loads Considering Non-Simultaneity—, *Central Research Institute of Electric Power Industry Report*, U92005, 1992 (in Japanese).

(Original Japanese Paper Published: November, 2021)
(English Version Submitted: February 3, 2023)
(English Version Accepted: February 24, 2023)